GERMAN-MONGOLIAN INSTITUTE FOR RESOURCES AND TECHNOLOGY

The present work was submitted to the Faculty of Engineering

Real-time volumetric measurement of grinding media of SAG mill

Bachelor Thesis

By

Nauryzbyek Byekyetkhan

Student ID: 14405685165071

Supervisor 1 / Examiner 1: Prof. Dr. Ariunbolor Purvee

Supervisor 1 / Examiner 1: Prof. Dr. Sungchil Lee

Advisor: Senior Engineer at OT Munkhbaatar Purevdash

Ulaanbaatar/Nalaikh,

8th of June, 2020

Statutory Declaration

Byekyetkhan, Nauryzbye	14405685165071
Last Name, First Name	Student ID Number

I hereby affirm in lieu of an oath that I provided the submitted bachelor thesis

xxx

I did not use any sources other than those stated. In case that the work is additionally submitted on a data medium, I declare that the written and the electronic form are completely identical. The work was not submitted in the same or similar form to any examination authority.

Place, Date	Signature

Abstract

This research work aimed to investigate the “Real-time volumetric measurement of grinding media of semi-autogenous (SAG) mill” by using an online-based model. Oyu Tolgoi (OT) mine copper concentrator is located in South Gobi province, south part of Mongolia. SAG mills are often taken as the object of optimization studies because they are a type of equipment that consumes large amounts of energy. Its size reduction stage includes one primary crusher which feeds two SAG mills (11.58m diameter x 7m length) with the following three ball mills (7.32m diameter x 11.32m length). After sag mill, comminuted products pass through a trommel screen in which over and undersize materials its oversize part is circulated into SAG mill and undersize part is conveyed to hydro-cyclone to further process.

The primary objective of this research is to discover viable measurement methods to determine an online ball charge level. Ball filling observation was implemented in this work using the mill’s load sampling and power draw. These methods could estimate ball filling variation with easy, undeniable, and based on available data at OT mine. We have estimated the correlation coefficient of power-draw and SAG load because it has a remarked relevance than other parameters. Afterward, to find more accurate dependency, at different conditions correlation coefficient is estimated.

The result obtained from this work show, the ball filling percentage variation is between 5 tons 25 tons which is quite well values according to the designed conditions. Besides, these ranges also classified three ranges based on the correlation determination value of R-squared value.

Key words: semi-autogenous mill (SAG), comminution, trommel screen, concentrator, coefficient of correlation, r-squared.

Table of Contents

List of Figures

Terminology

Aspect Ratio - (D/L) common convention generally refers to the high-aspect-ratio mill as SAG mill with diameter to effective grinding length ratios of 3:1 to 1:1

Toe position – this is the shell position, where the charge comes in contact with the mill liner.

Shoulder position – this the place on the mill shell, from which the mill load departs to the toe position

The mill charge – consists of a mixture of slurry and grinding media.

Grinding media – refers to the steel balls and large rocks used to break the ore

Slurry – refers to the mixture of water and ore material exhibiting the same flow properties as water.

Sensomag sensor – The Sensomag sensor is a device used to continuously measure both ball loading and slurry position within the running mill.

Volumetric filling – volumetric filling represents the fraction of the total mill volume occupied with a load.

RoM ball mill – ball mill Run-of-Mine (RoM) is a type of mill that uses steel balls between 30-35 percent and part of the coarse rocks at the comminution charge

Critical speed – critical speed is the theoretical rotation rate for the mil at which mill centrifugation charge

Centrifuging – it occurs at a speed of more than 100% of the critical speed. The outermost charging layer, which is in contact with the shell of the mill, rotates with the mill shell.

Grind-out – grind-out is performed to get rid of in charge materials form slurry and rock.

Cataracting – it occurs at mill speed above 80 percent of critical speed. A fraction of the charge is lifted high in the mill and dropped down to the toe position.

Cascading – this happens at mill speed below 60 percent of the critical speed. The material for the charge emerged from the shoulder of load, then it rolls down the freeload surface to the toe of the load.

Preface/Acknowledgment

I would like to express my deep gratitude to the GMIT Engineering Faculty and Oyu Tolgoi LLC for giving me the great opportunity to apply my acquired knowledge to real-life problems. The successful completion of this study was not possible without the participation and assistance of people that surround me such as supervisors, professors, and engineers from the company.

Especially, I would appreciate my supervisors Professor Ph.D. Ariunbolor Purvee and Ph.D. Sungchil Lee for their guidance, assistance, and patience in helping undertake this work. Their persistent, continuous guidance, advice, and support during this research. I would also express my thanks for their valuable feedback and suggestions.

It would like to gratefully recognize my research advisor Senior Engineer Advanced Process Control Munkhbaatar Purevdash from the company who was helping and sharing his useful ideas and suggestions. He also helped us by providing accessible data and information for doing research analysis. I would like to forward my acknowledgments to all my graduate colleagues and my team members for their assistance and feedback, sweaty memories.

Lastly, but not least, I would like to thank my family and friends for all the understanding for all the inconvenience and support during the completion of this bachelor thesis. Their persistent, continuous guidance, advice, and support during this research.

Chapter 1: Introduction

Mineral processing is the important stage in the mining chain which is the process of separating or liberating valuable minerals from the ores. Different types of minerals obtained from nature to separate valuable minerals by searching ore deposits. Firstly, the rock or ROM ore is extracted from the ore deposits, then it is transported to the stockpile area before that the bulk materials are crushed by primary crushers (cone crusher, jaw crusher). Secondly, these crushed materials are transported to the SAG mills by conveyors. After that, the grinding process takes place within SAG mill and it has a significant role in the processing plant, to which the current study especially relates. The function of the grinding is of course to ease as much as possible the stage of the process. The processed ores are further directed toward enrichment. For example, enrichment may be performed as floatation, in which water and floatation chemicals are applied to the soil. Each mineral has its favored chemical, which is added by the desired valuable mineral to the surface of the bubbles which form. By concentrating and filtering in, extraneous water is separated from the enriched product.

Mills used for grinding are usually cylindrical, in which water and the necessary grinder components are used to help in grinding, in addition to the ore itself. The grinder pieces can be rods, balls, or even large blocks of ore themselves can act as grinding material prices. Grinding is an important unit activity in the mineral processing industry that affects downstream process output such as leaching and flotation (Sarpong Bismark Donkor, 2014). As shown in Figure 1 tumbling mills are the most energy-intensive process in mining and it consumes more than 50% of the total energy in the mining chain (H, Wilber Churata). The term SAG is an acronym for semi-autogenous grinding. A fully autogenous mill uses the action of ore upon ore to reduce size. SAG mill uses the ore itself plus steel balls in the process to reduce the ore size. SAG mill is a large cylindrical vessel supported at each end (a feed end and a discharge end) by a hollow trunnion. There are grates at the end discharge end of the mill lining. These grates have small slots that allow slurry containing ore of a sufficiently small size to pass through. Between the grates and the end wall, or head, of the mills a cavity. The slurry flows through the grates into the cavity. And then out thought the discharge-end trunnion. Ore, water, and sometimes slaked

lime – forming a slurry of about 65-70 (ore and lime) percent solids – are fed into the mill through a retractable feed chute as the mill rotates. The slurry and the grinding balls together are referred to as the mill charge.

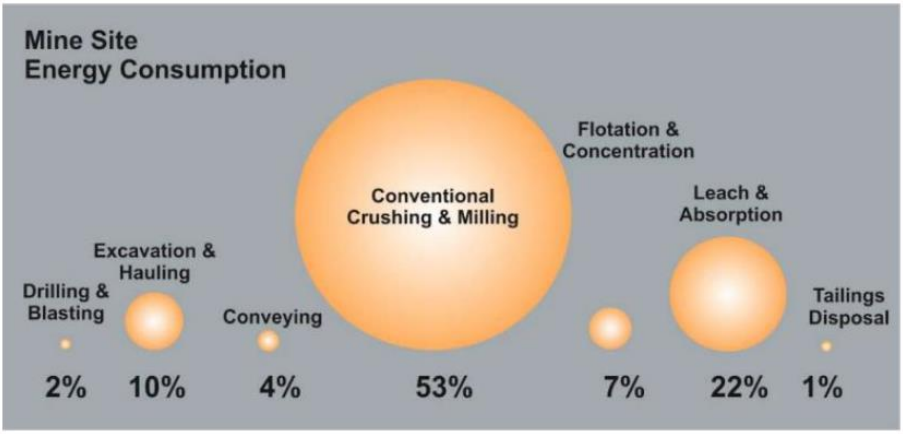

Figure 1. 1 – Distribution of energy consumption at a typical mine

The “OT” SAG mill charge takes up to 33-35 percent of the mill volume. Grinding balls occupy up to 18-20 percent of the mill volume and the ball movement inside a mill demands high energy. In a SAG mill, it is essential to maintain the highest impact energy to ensure the highest mill performance. When this is accomplished the highest efficiency is met in terms of energy consumption (less energy = high production = high efficiency).

Semi-autogenous (SAG) mill is currently one of the best options in the field of mineral size reduction. It has comparative advantages, such as high production capacity, lower physical space requirements, and lower investment and maintenance costs compared to conventional circuits.

1.1 The Motivation of the Research

The scope of this study is to estimate on-line dynamic volumetric ball filling using the available power data and mill weight of the mill load instead of the conventional measurements after mill crash and grind-out. The current invention presents a method, apparatus, and computer program for estimating the ball fraction inside the ore material in a grinding mill as a

percentage by volume of the total mill volume. The method requires the exact measurement of the total mill fill level with some other parameters that are dependable to the fill level and ball charge.

The function of the grinding is of course to ease as much as possible the stage of the process. The processed ores are further directed toward enrichment. For example, enrichment may be performed as floatation, in which water and floatation chemicals are applied to the soil. Each mineral has its favored chemical, which is added by the desired valuable mineral to the surface of the bubbles which form. By concentrating and filtering in, extraneous water is separated from the enriched product.

Mills used for grinding are usually cylindrical, in which water and the necessary grinder components are used to help in grinding, in addition to the ore itself. The grinder pieces can be rods, balls, or even large blocks of ore themselves can act as grinding material prices. Grinding is an important unit activity in the mineral processing industry that affects downstream process output such as leaching and flotation (Sarpong Bismark Donkor, 2014). As shown in Figure 1 tumbling mills are the most energy-intensive process in mining and it consumes more than 50% of the total energy in the mining chain (H, Wilber Churata). Several variables such as rotation speed, feed size, ball load, ball size, and volumetric filling affect a tumbling mill's throughput and efficiency. The main variable in this research is volumetric filling, which is the ball fraction by its volume in the grinding mill. The movement of balls within a mill requires high energy. In a SAG mill, maintaining the highest energy impact, to ensure the highest performance of the mill is necessary, the highest efficiency in terms of energy consumption is achieved when this is done (less energy = high output = high efficiency). Hence, to ensure this performance, it is important to maintain the ball charge level at the optimum point (H, Wilber Churata).

The common method on the plant to measure volumetric filling is by taking usual measurements after mill crash-stop. The crash stop for the mill involves operating the tumbling mill in a steady state by stopping all feed inlets into the mill and turning off the motor for the mill. Due to the mill downtime involved, this approach is destructive in output (Clermont et al., 2010).

Researchers have indicated that there is a strong correlation between power draw, mill weight, and volumetric filling. For instance, plant operators typically use mill power readings as a measure of the degree of ball filling and sometimes seek to hold it to the highest level. The absorbed power of the mill is well known to rely on operating parameters other than ball charges, such as pulp density and liner configuration. As shown in Figure 2 there is no linear

relation between the absorbed power of the mill and the degree of ball filling. As indicated on the graph, the result of a significant variation in the degree of balls filling could be a small variation in power. Since the wear rate of the ball depends directly on the media charge surface, a slight difference in power can result in a noticeable wear rate increase. An additional consideration is the risk of overloading and underloading the mill. Therefore, it is extremely important to have a precise measurement of the ball level in the mill (Clermont et al., 2010). Therefore, it is extremely important to have a precise measurement of the ball level in the mill, more reliable than power measurements, as well as a monitor of it.

In the present time, different techniques and computer simulation packages have been developed to measure and study mill charge behavior. Even though some of those techniques pose problems for plant operators. Firstly, the information received is in the raw state that must be fed into a control system before action can be taken. Secondly, in some cases, the signal containing the information relating to the grinding process remains hidden in the raw state, which involves specific detailed signal interpretations. While essential computer simulation packages only help to understand the influence of dynamic behavior on mill performance although they cannot be applied to industrial and pilot-scale mill operations (Sarpong Bismark Donkor, 2014).

To overcome these limitations, this works aims to use operating parameters such as power draw, total mill weight in the SAG mill to estimate ball fraction by its volume. These are potentially key features of volumetric filling estimation. The online measurement of ball fraction of the mill charge can be used as a tool by plant operators to make time-decision on abnormal alerts such as variations in the total charge level. The knowledge obtained would improve the efficient grinding circuit control and optimization.

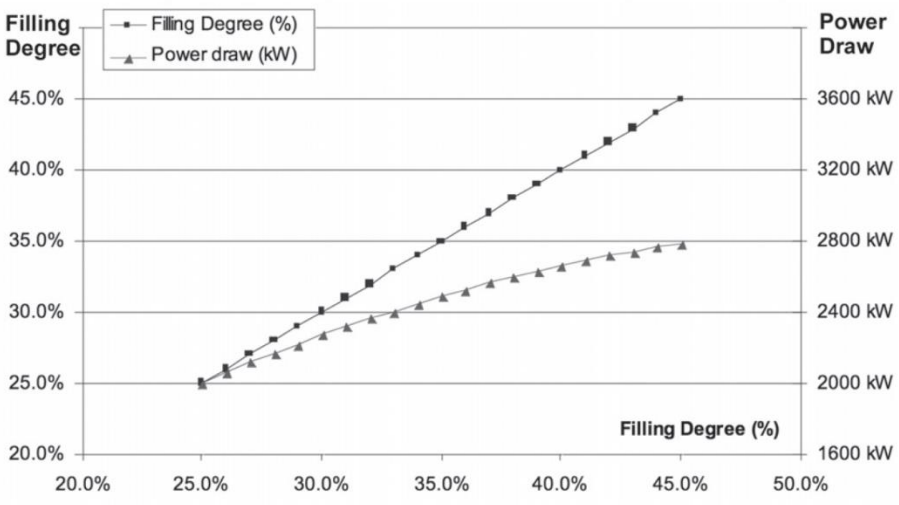

Figure 1. 2 - Nonlinear relationship between power draw and filling degree

1.2 Problem Statement

The mill fill level should principally be measured in different ways. However, problems with these have arisen in practical implementation. Methods by which fill level estimation is the known art used quite a little.

The present state of the art on attempts to measure the ball fraction has focused on especially gathering empirical data (power and mill weight) in running mills and measurements obtained from the process and process models are used. The invention involves the exact measurement of the fill level of the mill and some other measurement which depends on the filling level and the ball charge.

The method utilized in this patent is based on longitudinal lifters around the mill's circumference which strike the material inside the mill to be ground. The toe angle (the striking point on the longitudinal lifters) depends on the fill level and rotation speed of the mill (Bureau, 2011). Because of the materials strikes against the longitudinal lifters, oscillation is directed to the power or torque requisite to rotate the mill. It means when the toe angle shifts, the oscillation stage changes. Additionally, in the method of the invention, compensation is made for the fluctuation in the speed of the mill. The toe angle of the load is described by utilizing the information regarding rotation speed, the fill level can be estimated using some applicable mathematical models.

The proposed study aimed to bridge the gap between the two existing approaches: operating plant data collection and computer programming. Therefore, the principle of the present invention applied to measure ball charge is especially well suited for computerized seeking optimal state estimates. The method operates according to a recursive theory, in which measurement effects can be managed when process information is obtained, and the history of the measurement does not necessarily need to be stored. The estimation is carried out in a preferred embodiment by the control logic, in which the steps of the method are approached as a computer program. Finally, it is one of the viable-solution based on the available operating empirical data.

1.3 The Objective of the Research

The purpose of this thesis is first, to estimate the volumetric filling of the mill from the available power draw and the total weight of the mill inventories. Secondly, to determine ball fraction by its volume via on-line in the running mill using the mill empirical data and measurement and process models such as computer programming.

Chapter 2: Literature Review

Introduction

The overview of this chapter is to include an overview of the literature relating to the different methods used to study the dynamic behavior of the charge and fraction of each material in the tumbling mill. Detailed knowledge about the general use application and the types of tumbling mill used in the mineral processing industry is introduced. Tumbling mill is also considered the subject of optimization studies, as they are a type of device which consumes large amounts of energy. Among current developments, mathematical modeling and computer programming offer great methods for conducting these because of its low-cost performance, time-saving and reliability.

2.1 General Application of Tumbling Mills

Tumbling mill are commonly used in cement, pharmaceutical, and paint as well as particularly in the mineral processing industries for both coarse and fine grinding (Sarpong Bismark Donkor, 2014). Tumbling mills are composed of cylindrical shells, with sometimes a conical section at the end of feed and discharge and liners are attached to lifting elements of a surface shell (Wills and Napier-Munn et al., 2006). The shell of the mill rotates on its axis with hollow trunnions attached to the end walls. The larger mill diameter is usually needed to grind larger feed sizes. The mill's volume and efficiency depend on the mill's length concerning its diameter.

Tumbling mills can be used to reduce feed sizes from 5 mm and 250 mm to 40 – 300 μm (Napier-Munn et al., 2006). The rocks as ore, water, and steel balls are included in the charge material. With a certain speed, the tumbling mill rotates and the media and particles collide with each other to reduce size. Although, Autogenous (AG) and semi-autogenous (SAG) mills often operate in an unstable state, due to the difficulty of balancing the rate of replenishment with consumption of large ore particles from the feed-in charge (Jonsén, Pär, et al., 2011). The grinding process can be taken placed in wet and dry conditions, in either batch or continuous modes. In the continuous grinding, the feed material enters the inlet of the mill and discharges

the opposite side of the mill. On the batch process, a specific amount of material enters the mill, and the process takes a specific time then it discharges.

Cost-effective comminution is typically determined by mill design (mill, diameter, rotational speed, liner configuration), grinding media (hardness, density, chemistry, microstructure, etc.) and process control (feed rate (water, ball, ore), material size). A number of operating key parameters related to the operation of tumbling mills are discussed in the following sections, with a focus on their impact on the efficiency of the mill.

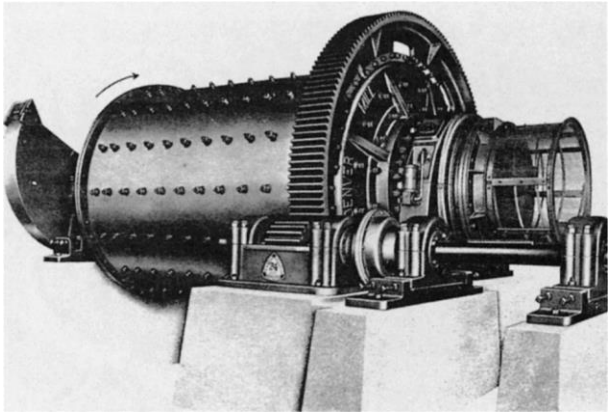

Figure 2. 2 – Tumbling mill symbol

Figure 2. 1 – Tumbling mill in Industry

2.2 Types of Tumbling Mills

The application of tumbling mills is various based on their functioning principles. There are four different mills according to the types of grinding media used for comminuting the materials. This consists of autogenous mills (SAG), semi-autogenous mills (SAG), ball mills, and rod mills.

Nowadays, the design of tumbling mills has improved in terms of mechanical performance and reliability, however, they are incredibly inefficient form the point of view of energy use. This can be understood as the most of forces involved in breaking the ore in grinding mills are from repetitive and random impact, which break not only liberated materials but also unliberated particles (Usman and Husni).

2.2.1 Autogenous (AG) mills

In autogenous mills, the feed is only ore itself and which can notably change its size. Inside a mill, large stone blocks and small pieces of crushed stones roll around in the mill and collide one another. Otherwise, it uses the action of ore upon ore to reduce its size and smaller rock material is created. When the material is sufficiently small enough, it passes through the discharge opening of the mill and at the same time new ore materials added constantly. However, the weakness of a fully autogenous mill is that it creates a comparably large amount of critical size rock matter.

2.2.2 Semi-Autogenous (SAG) Mills

In semi-autogenous mills, the feed is that ore itself, in addition to this water and steel balls to speed up the grinding process. The specific gravity of steel balls should be greater the average specific gravity of the rest of the materials and it is generally 2-3 times. The material of the balls are typically high-strength iron and steel. That's why, the balls occupy a large portion of the costs in the gridding process and it is not a good idea, to add a much amount of ball the mill. Moreover, if there are too many balls in the well-functioning mill, they increase unnecessarily power from the motor. A semi-autogenous mill is generally used for the primary grinding process. It utilizes between 6-18% steel balls (Spencer et al., 1999) and the range depends on ore behavior. SAG mill is featured with its short length and large diameter.

Semi-autogenous grinding (SAG) is one of the most widely used comminution methods. The plant (Fig 3) comprises feed as large pieces of rock and water into a grinding mill of various meters of diameter containing steel balls that rotate at a fraction of its critical speed. Containing the slurry and the ball adheres to the mill's walls before being cascaded. A given angle, causing impact and thus fragmentation of ore (Núñez, Felipe, et al., 2011).

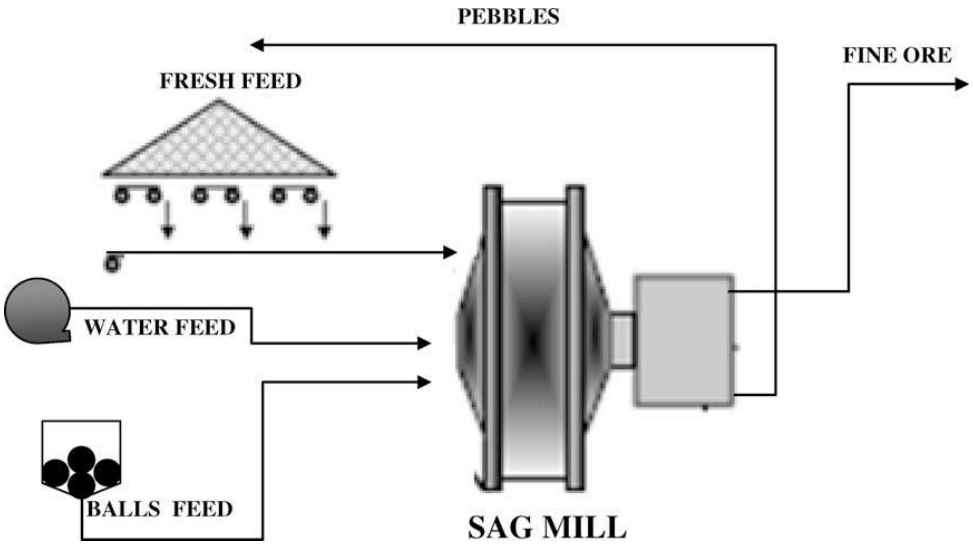

Figure 2. 3 – Example of a typical configuration of SAG milling

2.2.3 Ball Mill

Ball mill is generally used for the secondary grinding process. The steel balls are the main portion of grinding media, which can be between 30-40% of the total mill volume. In this case, grinding is carried out by the ball. The input ore size for the ball mill is about 1 millimeter and a result a powder-like material produced. Ball mill characterized by a smaller diameter and long length as compared to SAG mill (Napier-Munn et al., 1996; Will, 2006).

2.3 The motion of the Charge in the Tumbling Mills

The peculiar characteristic of tumbling mill is the use of loose crushing bodies, which are large, hard, and heavy in corresponding to the ore particles, but small in comparison to the mill volume, and occupying (including voids) slightly less than the volume of the mill. Because of the mill shell rotation and friction, the grinding medium is elevated from the rising side of the mill until a position of dynamic equilibrium is reached (the shoulder), when the bodies cascade and cataract down the other free surface, about the dead zone where little movements take place, down to the toe of the mill charge (Napier-Munn, et.al., 2006).

Cascading motion happens at low speed, where the load rises to a certain height along with the shell and rolls free area of mill to the toe region of the charge. The cataracting movement happens at high speeds but lower than critical velocity. The load leaving the shoulder

area assumes a parabolic path before rolling down to the toe area (Figure 2.4). The shape of the load is determined from the movement inside the tumbling mill. The driving force of the mill is transmitted to the load via the liner. At significantly low speed and with smooth liners medium tends to roll down to the charge's toe and the comminution is abrasive. The cascading movement leads to finer grinding but increased liner wear. At higher speeds, the medium is projected clearly to create a series of parabolas before landing on the toe of charge. The cataracting leads the coarser product and less wear on the liner. Centrifuging occurs at the critical speed of the mill and the medium is carried around in an essentially fixed position against the shell (Wills, Napier-Munn, et.al., 2006).

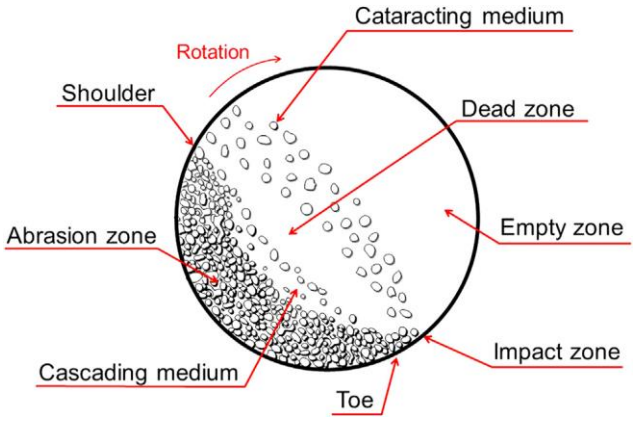

Figure 2. 4 – Motion of charge in a tumbling mill

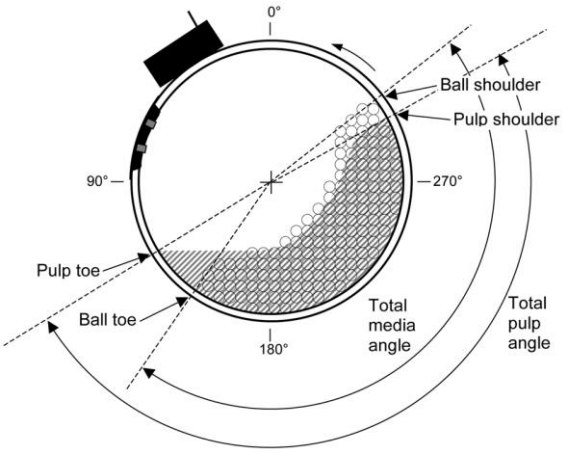

Figure 2. 5 – Cross-section of the mill with angular references

2.3.1 Speed in the tumbling

Control of speed in an operating mill is essential, as speed affects motion behavior, power draw, product size, and wear of the liner and ball. The driving force of the mill is transmitted to the load via the liner. At significantly low speed and with smooth liners medium tends to roll down to the charge's toe and the comminution is abrasive. The cascading movement leads to finer grinding but increased liner wear. At higher speeds, the medium is projected clearly to create a series of parabolas before landing on the toe of charge. The cataracting leads the coarser product and less wear on the liner (Wills, Napier-Munn, et.al., 2006).

Centrifuging occurs at the critical speed of the mill and the medium is carried around in an essentially fixed position against the shell. The following formula is used to determine the critical speed of mill:

$$N_c = \frac{42.3}{\sqrt{D-d}} \text{ [rev/min]}; \quad (2.1)$$

Where N_c is the critical speed of the mill, D is the mill diameter in meters, d is the ball diameter in meters. The equation assumes that there is n slip between the medium and the shell liner. In practice, the magnitude of the estimated critical speed is usually increased by around 20%. In general, the mills can operate at 70 – 80% of the critical speed.

2.3.2 Grinding Media and Mill Loading

Ball-filling play an important role in a grinding-circuits and one of the essential factors that affect the mill's throughput and performance. Optimal grinding media can improve milling efficiency and reduce operating costs. Grinding media are used in different grinding environments involving SAG, rod, conventional ball, and tower mills. Commonly, grinding ball made of heat-treated and as-rolled grinding rods, cast steel and cast iron, as well as forged steels. The martensitic low alloy steel is also commonly used today, because of its low cost and improved wear/abrasive resistance. Wear resistance and milling efficiency are used as an indicator for the assessment of the grinding media effectiveness. Wear resistance depends on the selection of alloys, the operation of the milling process, and the environment of the mill (Sarpong Bismark Donkor, 2014).

Selections of media size, shaping factors, and the nature of media are aspects that affect grinding results. To achieve optimum mill performance, the essential variables involving size, mass, hardness profile, and chemistry must be properly designed, specified, and controlled. Small defects in properties or quality have apparently a strong impact on grinding performance. Large variations in properties could be found on grinding media designed by various manufacturers. Ball quality control may be used as useful instruments to conduct precise measurements with some degree of confidence.

Steel balls have a significant impact on the performance of the mill since the specific gravity of steel and its hardness are also relatively greater than (7.8 – 8.0) that most of the ores (2.5 – 4.5); hence they can produce such large kinetic energy that makes them very effective, especially for impact breakage (Napier-Munn, et.al., 1996). The presence of grinding ball within

a mill will increase the impact on breakage and, therefore break the larger rocks very faster. Since more energy is required to crack bigger rocks, greater balls need to be used to hit them.

The ball sizes used in tumbling mills depend on the hardness of the ores and the distribution of the size of the feed for breaking. It is important to apply balls used in SAG mills in such a way that the largest balls are only heavy enough to smash the largest and hardest particles in the feed. Ball required for the coarse and hard ores are larger than those needed for fine and soft ores. The inclusion of steel balls allows for more rapid breakage of coarser material. If the ball charge is up to 12% and the size of the ball is increased then the breakage rate will increase in the coarser size ranges, on the other hand, will decrease in the lower size ranges.

At the operational level, it is typical for SAG/AG mills with trunnion discharge to use a maximum mill load of approximately 35%, while the charge range for a mill with end-discharge designs is usually between 40 and 50% (Rowland, 1998).

2.3.3 Influence of Ball Charge on Mill Performance

Tumbling mill performance is very sensitive to the volumetric mill filling that influences wear rates on grinding media, throughput, power draw, and product size, etc. A pilot plant experiment has conducted with an overflow discharge mill, is seems that the pool size has an also major influence on the grinding rate. Therefore, inventories of the mill are consequently main process variables, and obtaining a measurement of these parameters will provide means for their control. Improving their controllability will in turn provide process improvement operations and then cost-effectiveness (Engineering, Chemical, et al., 2006).

2.3.4 Influence of Ore Characteristics in SAG Mill

Variation in the ore hardness fed to SAG mill mainly affects the output of the mill in terms of throughput. Ores that appear to have packing between liner spaces may affect shell liner performance. Increased grinding ball size will retain their milling rate for harder ores. Therefore, the liner design needs to be changed to allow the shell liner to withstand the greater impact forces of the larger ball size (Royston, 2008). In addition, pre-crushing can be used as the other way to treat harder ores to provide a feed that is more suitable to breakage in milling. Concerns related to the type and size of the should be predicted earlier because consistent ore

characteristics are critical in the case of SAG mills to make the mills work best. Some mine operators deliberately are the type of ore and prepare stockpiled with a constant mixture of ore.

Consistently, ore size and hardness have different influences on shell lifter wear. High milling throughputs with low lifter wear may be achieved if a softer ore doesn't result in packing. A fine, but hard, ore may produce high mill throughputs (without packing) but the abrasive liner wear is increasing. Both soft and fine ores are difficult to stick in the mill resulting in damage to the liner due to increased shell impacts form the ball-on-mill.

2.4 The Shape of the Charge in the Tumbling Mills

The charge movement inside the tumbling mill has been investigated by many researchers for both applications for wet and dry grinding. Rose and Sullivan discussed the charge's motion in a laboratory mill fitted with a transparent window for studying the dynamic condition that appears in a mill. The charge motion was described as a pendulum-like fluctuation of the whole load about the charge center. Those writer's work was limited to the dry grinding environment (Jonsén, Pär, et al., 2011). Figure 2.6

The highest position the charge is reached so-called "shoulder". The position is where the charge of the mill comes into contact with the shell of the mill. The charge's toe and shoulder positions are the boundaries of touch on the shell of the mill. These can be used to calculate mill volumetric filling and these are significant variables in the modeling of the mill control system.

2.4.1 The Methods for determining of the shape of the Charge

A number of researchers carried out experiments that included the extraction of the shape of the charge such as Moys, (1998), Morrell, (1993), and Powell (1995). Some of those people used various experimental techniques to test the shape of the charge. Measuring the shape of the load is essential for understanding the load dynamics in the grinding mill.

2.4.2 Morrell's charge shape

Morrell (1993) determined the shape of the charge movement using variable speed in a laboratory mill which is equipped with a glass window. Figure 2.5 demonstrates laboratory schematics used in mill research. The charging motion was filmed using a slower shutter camera by the edge of the glass. The effect of milling velocity and filling of the toe and shoulder angle of the mill was investigated. Snapshots of the motion of the charge is taken between 73 - 95% of critical speed and 15 – 45 % of mill volumetric filling.

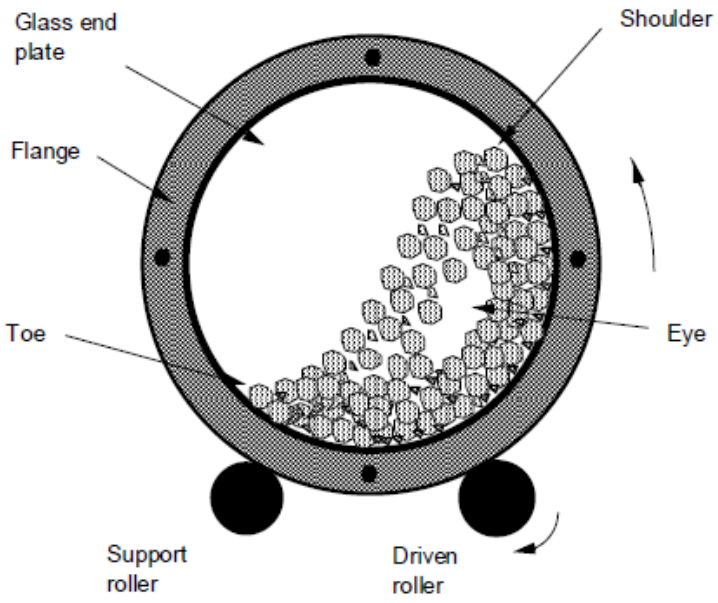

Figure 2. 6 – Schematic illustration of Laboratory mill with glass window

The general pattern of the charge, from the photographs of the laboratory mill that is as schematically shown in Figure 2.7. As the mill rotates the load is lifted up the upward face of the mill until reaching the shoulder. The bulk of the charge falls off toward the toe region at that point (shoulder). Moreover, the small size of materials are discharged as a 'spray' which impacts in some cases on the opposite face of the mill, directly onto the exposed liners (Morrell, S., 1993).

Measurements of the photographs were taken from the angular displacement of the shoulder and toe. A pictorial definition of such measures in conjunction with relevant symbols and system coordinates can be seen in Figure 2.7

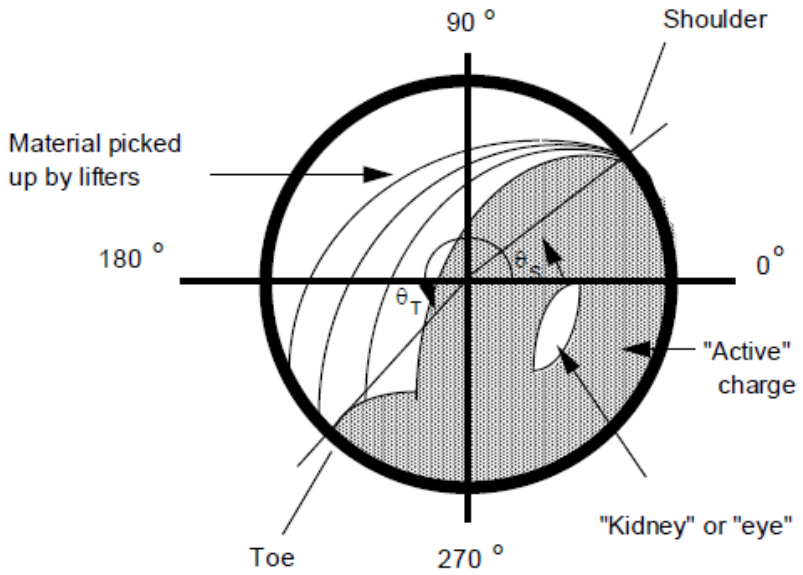

Figure 2. 7 – The shape of the Charge in the tumbling mill depicted by Morrell

Morrell proposed the following empirical equations relating the shoulder and toe angle of the load to the mill speed and volumetric filling based on experiments performed in the laboratory. The volumetric filling can be determined when the shoulder and toe region of the mill charge is known. Equations 2.2 – 2.4, to help measure the toe and the shoulder angles and the volumetric filling.

$$\Theta_S = \frac{\pi}{2} - (\Theta_T - \frac{\pi}{2})*((0.3386+0.1041\,\Phi_C) + (1.54 - 2.567\ \Phi_C)*J_t) \quad (2.2)$$

Equation 2.2 only used the toe position and the experimentally estimated fraction of the theoretical critical speed at which centrifuging is fully developed otherwise the critical speed of the mill.

$$\Theta_T = 2.5207*(1.2796 - J_t)*(1 - e^{-19.42(\varphi - \varphi c)}) + \frac{\pi}{2} \quad (2.3)$$

$$\varphi = \varphi c \qquad \varphi > 0.35*(3.64 - J_t) \tag{2.4}$$

$$\varphi c = 0.35*(3.64 - J_t), \quad \varphi \leq 0.35*(3.64 - J_t) \tag{2.5}$$

where:

J_t - is the volumetric filling

Φ - is the experimentally determined fraction of the theoretical critical speed in which centrifuging is fully developed.

φc - is the percentage of the critical speed, at which the mill is operated.

The angles of the toe and the shoulder were related to the operating variables of the mill, especially rotation speed and mill filling rate. Figure 2.8 and Figure 2.9 demonstrate the shoulder and toe variations with the filling changes and the speed of the mill, respectively. As the mill increased, the shoulder angle of the mill charge correspondingly raised. The change in shoulder angle was due to the expansion of the mill charge. Conversely, to an angle of toe declined with an increase in Morrell's mill filling.

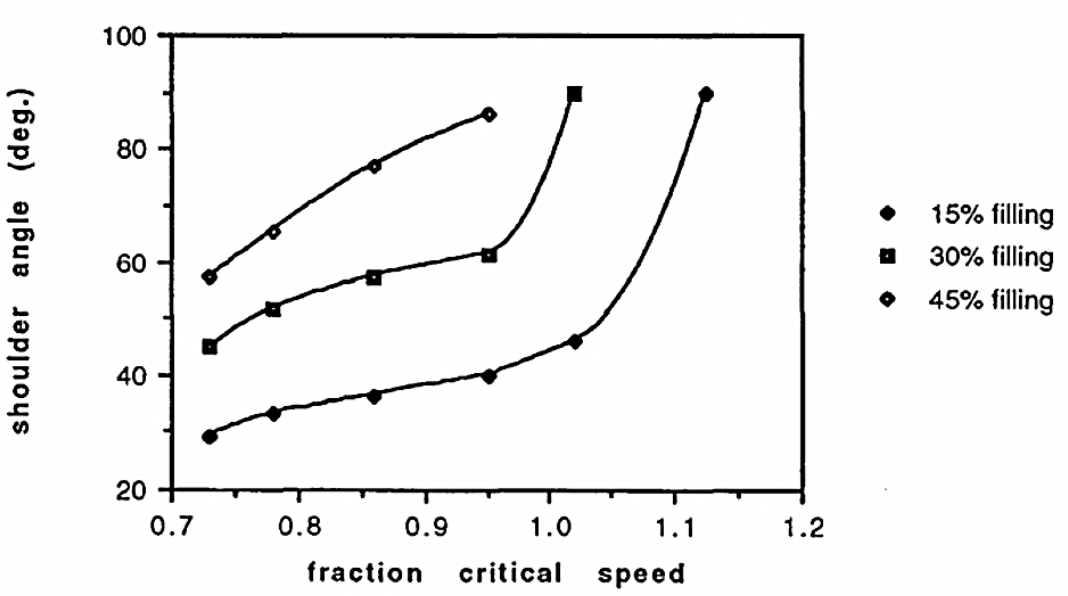

Figure 2. 8 – Shoulder Position Variation with Speed and Mill Filling by Morrell

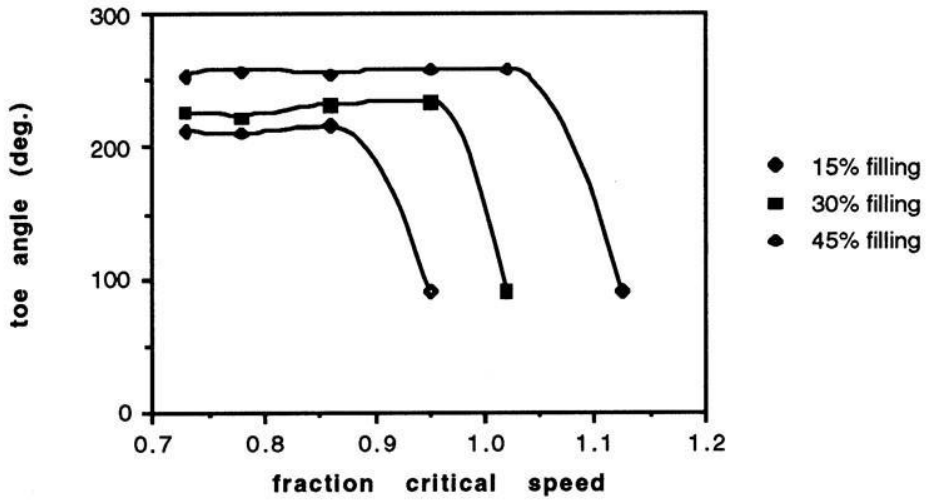

Figure 2. 9 – Toe position Variation with speed and mill filling by Morrell

As a result, the Morrell's has some limitations, the method of estimating the form of charge from the photographic snapshots are not acceptable to large scale mills because of the harsh conditions that prevailing within the mill. Moreover, the toe and shoulder regions cannot be determined online. Although, with advanced technologies, improvements can be made, which would enable direct measurement behavior within industrial mills. Discrete Elements Method (DEM) simulation gives a great opportunity to a better understanding of charge trajectory and more detailed about developing improvements reviewed next sections.

2.4.3 Discrete Element Method

The simulation problem with the tumbling mill as intractable due to the multiparticle collision actions involving thousands of balls and rocks. The strict environment inside the mill prohibits any measuring sensor interference. Physical models are simpler with some empiricism unable to accurately identify load movement inside the mill. The system of the discrete element method (DEM) provides a viable solution to this problem.

The DEM is a common tool for analyzing particle flow, and DEM grinding process simulation can aid in the study of grinding mechanism and formulate reasonable decisions and predictions. From theoretical and experimental points of view, the mixed motion of the steel balls both falling and dropping is analyzed, this analysis shows different grinding requirements can be met by selecting the appropriate rotational speed and ball charge ratio (Owen et al., 2015).

Cundall and Strack (1979) seem to be first to propose DEM for analysis of rock mechanics. The usage was by Mishra and Rajamani et al (1992, 1994), the DEM to study charge movement in the tumbling mill. DEM has extensively employed extract load shape features and many researchers to study charge motion in 2D and 3D for the prediction of charge shape and charging trajectory in the industrial mill (Moys et al., 1994). It was also used to predict the movement of charge, the power, segregation, and wear rates in ball mills as well as charge motion in rotary mills. Usage of DEM is expensive, because of computing costs are involved. Only part breakage of the content is not included in most of the DEM codes for tumbling mills that make it difficult to estimate the impact of charge characteristics on the mill performance. Therefore, this has led to an interest to study sensor technology.

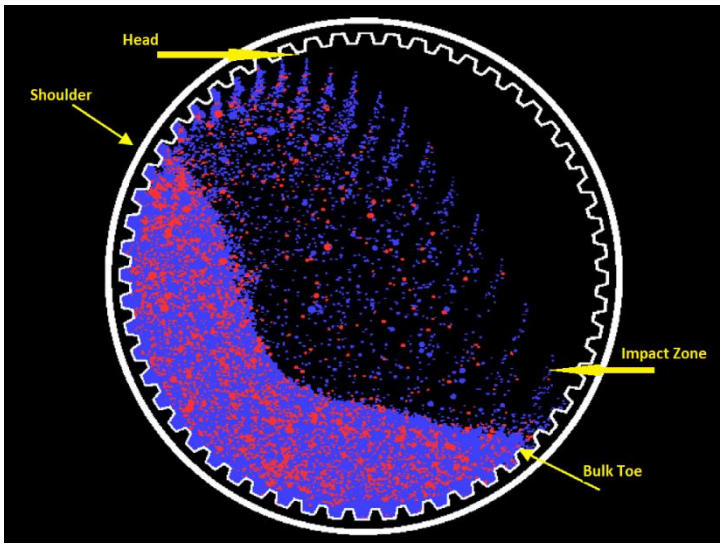

Figure 2. 10 – Standard particle visualization showing location of bulk toe and shoulder. The rocks are shown as blue and the balls are red.

Visualizations of the shape of the charge and the pattern of the streak were used for determining the impacted toe, bulk toe, shoulder, and head regions. Standard visualization of DEM particles, as seen in Figure 2.10, was used to estimate the locations of the bulk toe and shoulder. Streak patterns, as indicated in Figure 2.10 for the calculation of impact toe and head locations. A representation of as streak is formed by tracing the trajectory of each particle position over a specific time interval which is 0.2 s in this case. Then the streak patterns represent the motion of the charge while a standard rendering of the particles only the current location is shown. This enables that to identify the cataracting stream and shape of the bulk

charge as well as improves the accuracy of the identification of the shoulder angle (Owen, Phil, et al., 2015).

2.5 Load Behavior Measuring Technologies for Tumbling Mill

Various methods for analyzing the dynamics of the system have been proposed over the last decade to measure the charging behavior of tumbling mills. Usage of the different sensors and, particularly, a sound sensor for the calculation of the toe and shoulder position of the mill load, and it is more detailed next sections. Methods do determine the dynamic behavior of charge within in the mill classified two types: on-shell or off-shell method (Sarpong Bismark Donkor, 2014). On-shell sensors rotate with the running mill and are capable of providing detailed and direct information about the state of the process at each point on the mill shell. The on-shell method comprises the following tools; such as the conductivity probe, the piezoelectric strain transducer, the strain gauge, and the Sensomag sensor.

2.5.1 Conductivity Probe Technology

The conductivity probe comprises two main components which are an anode and a cathode electrode. The probe tests the conductivity of fluids when a voltage is applied over it. Due to the force of voltage, the negatively charged ions move to the anode, while the positive ions move to the cathode. These ion movements are a measure of conductivity. The conductivity probe used in the mineral industries for measuring slurry density and shoulder position of load within the mill.

Moys (1985), Herbst (1988), and Gabrdi (1998) carried out pioneering work in the dynamic development of sensors, probe conductivity, and also in the application of those tools to the control of grinding mills. Moys and Montini (1987) showed that conductivity measurements well describe the load-behavior is strongly influenced by the rheology of slurry. Moys declared They studied the actions of the mill loads as regard to toe and shoulder positions using a probe for laboratory mill. The prove was inserted into the liner bolts of the mill and the sensing face was parallel to the rotational milling axis. The probe was isolated from the liner and shell an epoxy coating to prevent the loss of the probe's electrical currents. The impacts of rotational speed and volumetric filling were estimated for the load behavior. Figure 2.11 shows a built-in conductivity test.

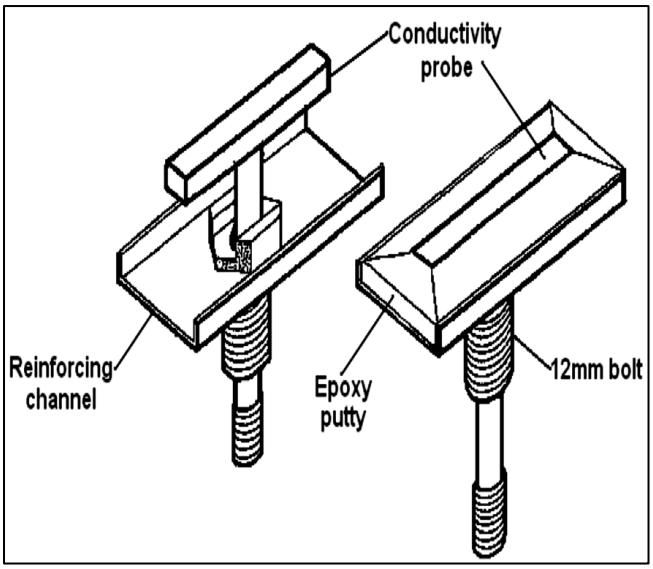

Figure 2. 11 – Conductivity Probe Built-in used by Moys et al., (1988)

2.5.2 Strain Gauge Sensors

The strain gauge sensors determine the strain of an object which means that measures the deflection of a lifter bar when it hits the charge inside a mill. Lifter bar deflection during mill revolution gives rise to a characteristic signal profile which shows information about both charge position and performance of grinding. A strain gauge can be made from a round and flat coil fasted to an object's surface. Strain gauges used for load cells, force, and torque sensors for controlling mill charges (Moys and Skopura, 1993).

As has been described that the strain gauge measures the deflection of a lifter bar inside a tumbling mill. Its deflection magnitude is a direct response to the grinding charge volume within the mill and also to some extent of the behavior of charge in grinding. The volume of charge and its movements have a strong effect to the performance of grinding and wearing the rate of mill liner. Consequently, the strain-gauge signal contains information and behavior of the grinding process. in monitoring process data, and in particular, where multi-sensor system data is available, the frequency of data collected may often reach several thousand levels each minute. This problem has become important in many aspects, for instance, historical data storage capacity, speed of on-line processing, and faster analysis and interpretation of data.

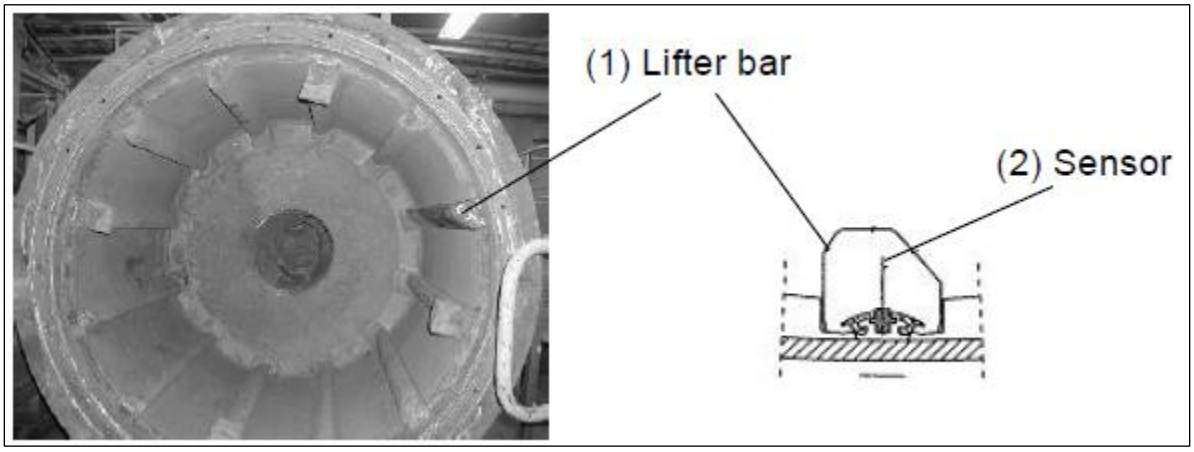

Figure 2. 12 – Pilot Mill showing the Lifter Bars where one of them has strain-gauge sensor by Tano et al., (2005)

The Continuous Charge Monitoring (CCM) system is a relatively new electronic measurement device developed. It is dedicated to the continuous calculation of the volume of charge provided that the mill has a rubber-metal lining mounted in the mill. As shown in Figure 2.12 the lifter bar is fitted with a strain gauge sensor which measures the lifter bar bending when it contacts the mill charge. The electrical signal is amplified from the sensor and sent to the receiver. The receiver has a trigger pulse remote sensor which is triggered once every rotation by a metal trigger plate on the mill. The lifter bar, trigger plate, and receiver position are carefully determined. The s signal from the receiver is sent to a computer system where the data is processed to indicated the level of charge and the angle of repose (Tano et al., 2005).

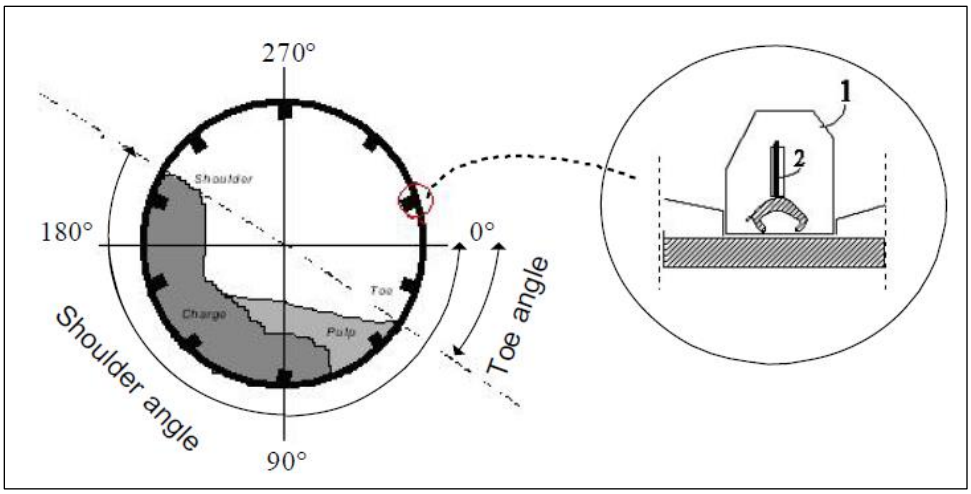

Figure 2. 13 – Simplified view of the Sensor, the part is a cross-section of a mill with a horizontal line, the right part is the lifter with a strain gauge

A general deflection profile of the sensor signal is shown and an attempt to break it into seven segments. In Figure 2.14 along with a corresponding schematic cross-section of a plant. The bounds and scale of the partitions are determined by the knowledge of the grinding process. each segment provided in Figure 2.14 illustrates a significant dynamic occurrence when the sensor-equipped lifter bar passes under the mill load. The ordinate in Figure 2.14 shows the lifter bar deflection, which corresponds indirectly to the force acting on it, and abscissa is the angle of rotation of the mill with a resolution of 1 degree.

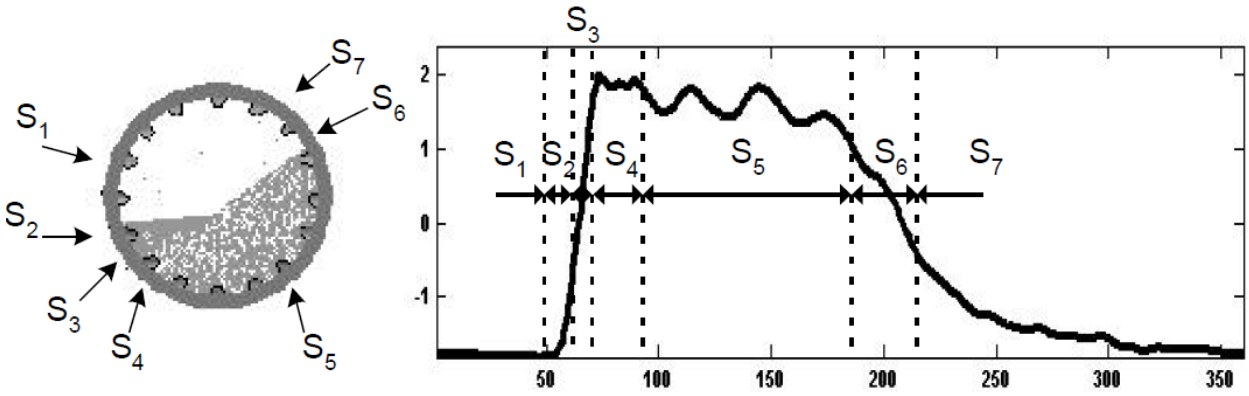

Figure 2. 14 – Segmentation of a typical signal during its passage in the charge sensor by Tano et al., (2005)

The sensor signature reflects various process characteristics such as mill load and mill load charging behavior. Both S2 (charge hit) and S6 (Charge left) segments are well known and can be used to calculate the charge, these data provide a fair measure of the position of the volumetric mill load and repose angle. The other segments are less known but are expected to carry the grinding efficiency information.

2.5.3 Inductive Proximity Probe

The Inductive Proximity Probe is made from a ferromagnetic coil that works based on the principle of induction. The ferromagnetic coil generates a magnetic field while the mill is rotating inside the mill and any steel balls that enter the magnetic field cause a variation in amplitude of the field. In the mineral processing industry, the inductive probe sensor was used for controlling mill conditions.

Kiangi et al (2006, 2011) measured the position of the toe and shoulder of the charge in a dry pilot mill with an inductive proximity sensor. Figure 2.15 demonstrates the inductive probe installation to the pilot mill. The effects of mill filling and mill speed on the toe and shoulder positions were investigated, as well as the net power. A series of studies conducted in a pilot plant with steel balls as grinding media and dry quartz as an ore. The inductive probe signal approximate media of toe and shoulder position.

Figure 2. 15 – Installation of the Inductive Proximity Probe on the Pilot mill

2.5.4 The Magotteaux Sensomag sensor

Professor Moys from the University of Witwatersrand in South Africa has published papers defining the slurry rheology effect and flow rate on mill behavior in 1988. The relationship between slurry and media had been emphasized by looking at the efficiency of the grinding mill. At the meantime, it was hard to gain a lot of useful information in an aggressive environment. Twenty years later the Sensomag was able to demonstrate this interaction by looking angle of median and pulp position (Clermont et al.,).

An innovative tool (Sensomag) that can lead to delivering information on running mills and it is developed by Magotteaux. This will provide a precise online measurement of the degree of grinding ball filling and location of the pulp for making timely decisions and taking action. This too can operate on its own and in conjunction with an automatic ball loading grinding system called Magoload. Consequently, ball load may be kept constant by direct utilization of real-time measurement. The Sensomag is composed of an inductive proximity switch and conductivity probe mounted as part of liner in a mill. The key data are described as

regard toe and shoulder angle. The density of the pulp is an important parameter that is affecting the performance of grinding. For instance, in iron ore, a variation of 2 – 3 % of the solid content in a slurry may result in up to 10% on the energy for the same grinding (Clermont et al.,).

The Sensomag's main element is a standard polyurethane beam that mounted inside the mill and containing sensors that measure the ball directly and the presence of slurry. There is no complex analysis of any indirect signals such as noise, shell vibration, and power draw. (Figures 2.16, 2.17.) The analysis of ball load and pulp is carried out on a mill section, at each revolution. Then those raw data are sent to a central unit by wireless connection where data are processed.

Figure 2. 17 – Example of Polyurethane Sensor Beams inside of mill shell

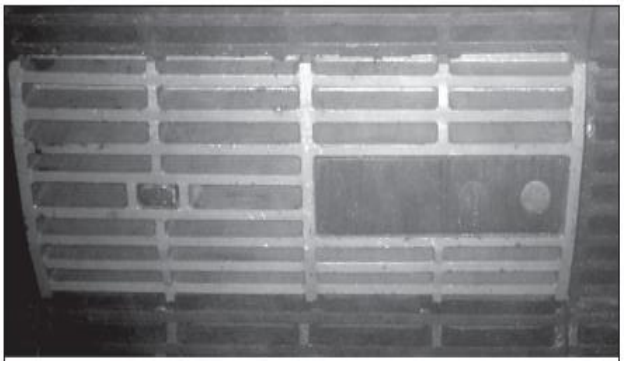

Figure 2. 16 – Example of Polyurethane Sensor Beams outside of mill shell

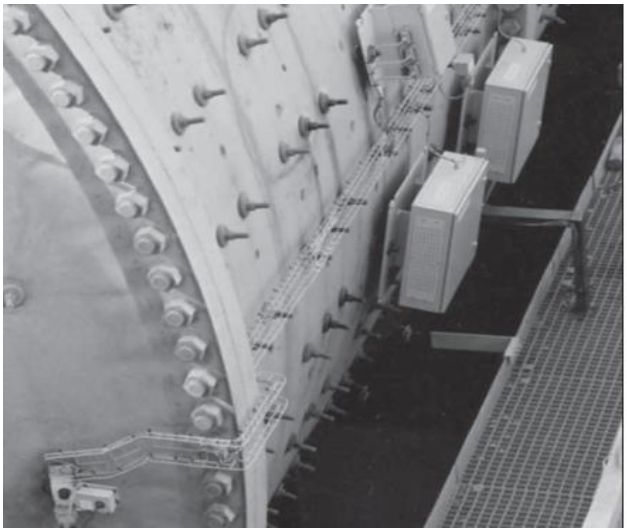

Figure 2. 18 – Installation of Sensomag System

The four angles are then calculated and made accessible via a standard online customer supervision system OPC link or electrical signals range of 4-20mA. (see Figure 2.18) As mentioned before, the information of ball load and slurry positions within a running mill is a great opportunity to maximize usage of equipment, leading the way increase in efficiency and throughput, as well as energy consumption and cost reduction. The Sensomag can also provide filling rate (in percentage volume) based on the different angles and mill absorbed power. It requires shut down at least one to perform a manual measurement of the ball filling degree to allow mathematical model for calibration. Once it calibrated, the Sensomag

can be utilized to accurately control steel ball consumption, manage ball additions, reduce shutdown time for grind outs and enhance safety by reducing the number of internal inspections of the mill.

2.5.5 "SAG Mill Online Ball Charge Level Measurement by Sound" at San Cristobal Mine

This study serves to solve the San Cristobal Mine's matter of optimal ball charge level in a SAG and Ball mills by using the mill sound and the mill bearing pressure as its main variables. In the paper, Wilber Churata aims to maximize efficiency as well as throughput whilst also decreasing energy consumption. The main parameters that are essential to the model created in this paper are pressure (charge mass), sound (charge level), and linear wear rate of mill. The overall results of the model were evaluated utilizing statistics regression using both a correlation coefficient and a root mean square error. From the data of the paper, it is observed that for the SAG mill the relative correlation coefficient was 0.70. However, the correlation coefficient was 0.90 and 0.78 in both ball mills showing that the relationship between pressure, sound, and ball charge levels is better in ball mills rather than SAG mills. The overall sound control system of the SAG mill at SCM had four microphones on each side of the mill.

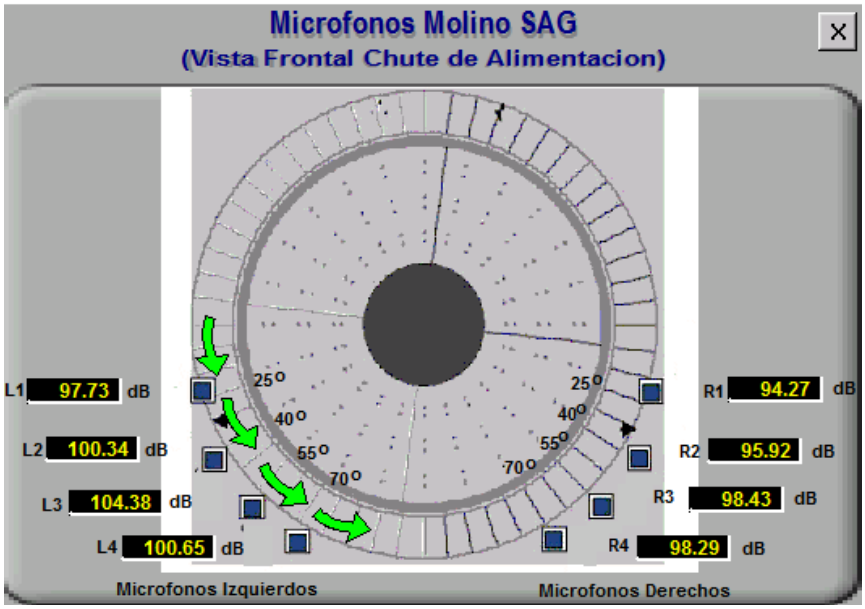

Figure 2. 19 – SAG mill sound at SCM, four microphones on each side of the mill

The optimizing control system (OCS) of the SAG mill manipulates feed rate and mill speed to maintain a specific sound set point that corresponds to the optimum impact point. The control of the sound set point means that the charge level is also tightly controlled which in turn allows for the charge mass variation to be determined by measuring bearing pressure. This correlation is what allows for the SAG mill to run at a constant ball charge ratio. There are two main equations, the first being Pressure [Specific dB] = Bearing Pressure [Specific dB] + wear rate. After establishing a regression line for the bearing pressure vs sound graph it is quite straightforward to determine the ball charge level. As a result, the ball charge model helps to cause an increase in the mill's throughput and grinding efficiency and reduction in energy consumption.

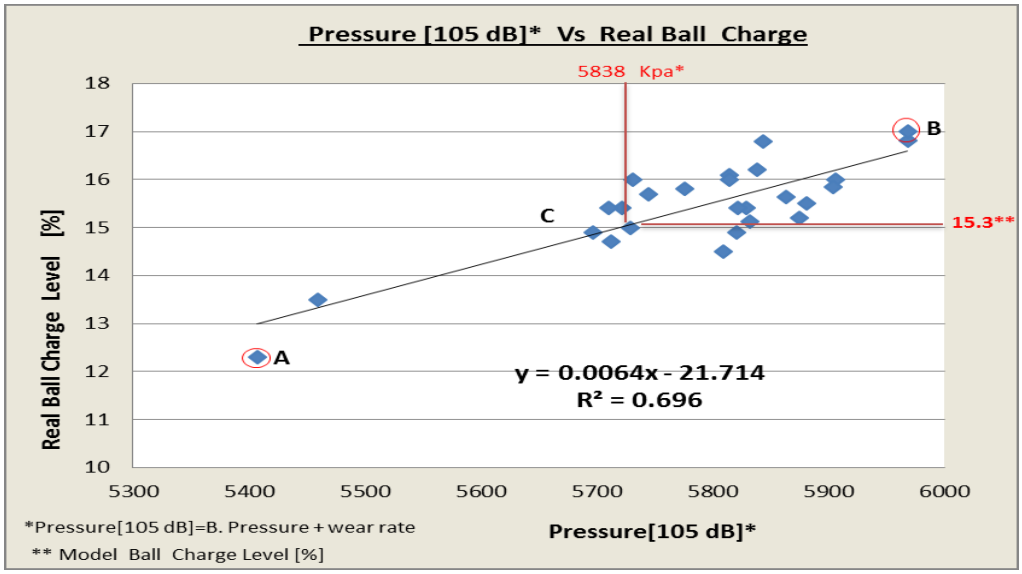

Figure 2. 20 – Regression Pressure [105 dB] vs Real Ball Charge

Considering the relationship between pressure [105 dB] and real ball charge by SAG mill grind-out and scan measurement, the variation in pressure [105 dB] on the direct correlation with ball charge level is determined (see Figure 2.20). The coefficient correlation values are R = 0.83 and the r-squared R^2 = 0.7. the result was successfully modeled by the following equation:

Model SAG mill: **Ball charge level = 0.0064*pressure [105 dB] -21.71.**

For this method to be implemented and work efficiently it is crucial to have the necessary data for the correlation of bearing pressure vs sound and real ball charge vs pressure. The flaws of this model include the need for a wide range of data for a precise approximation. The more data that is available for use, the more the precision will increase as the relative RMSE will decrease. Another flaw of this model is that it requires accurate sound readings. From the experiment data, we observed that the real ball charge and model ball charge can differ by at max 1-2% however this is also a big margin.

2.6 Conclusion

The use of online sensors and numerical methods to measure the load in a running mill has been revised. Much of the experiments were about how to estimate the load behavior of pilot-scale RoM ball mill and in a laboratory for dry milling applications. Though these sensors are used to provide information on the mill load behavior, there are few challenges relating to their application. The raw data obtained demands sophisticated mathematical representation of the information before the plant operator has used, then it would be meaningful. Some of these sensors aren't robust enough to withstand the severe environment inside an industrial mill.

Taking into account the above challenges, this study has used theoretical raw data proceeded in running mills such as power-draw, mill total weight, and feeds. Therefore, the correlation of the above data was analyzed for measuring the dynamic behavior of the charge within industrial scale mills. Then, these data were modeled mathematically for online measurements of the ball and slurry sizes.

Chapter 3: Experiments and Methods

Introduction

The chapter explains the description of models and methods that were used in this like simulation and data analysis involved in this study. Firstly, the experimental design detailing the Kalman filter algorithm for estimation and prediction especially data correlates with the system noise. Secondly, essential parameters of a synchronous motor which is rotating SAG mill and its effects on overall mill output is discussed in the next section.

After that, the correlation of theoretical data was measured during the running mill. in this section which parameter has more influence on the ball charge rate were discussed.

3.1 "OT" Grinding Process Circuit description

The research focuses on the grinding circuit of the Oyu Tolgoi copper-gold mine concentrator in the South Gobi region of Mongolia approximately 550 kilometers south of the capital Ulaanbaatar. The circuit treats approximately up to 4000 tph of high-grade of copper ore and consists of primary and secondary grinding circuits. The simplified primary grinding circuit is illustrated in Figure 1. The ore conveyed from the stockpile is fed to the SAG mill for primary grinding. SAG mill discharge products classified into two parts oversize and undersize by screens. The oversize materials go back to the gyratory cone crusher, while the undersize materials are mixed with water and fed to the primary cyclones for further classification. The primary cyclone comprises overflow and underflow products. The underflow product is separated by a small recycle one is fed to the SAG mill chute and the other one is to the ball mill feed stream. The production process goes through several stages, including ore crushing (gyratory cone crusher), grinding (SAG mill), size reduction (ball mill), classification (cyclones), and separation (flotation) where the concentrate is separated from natural rocks.

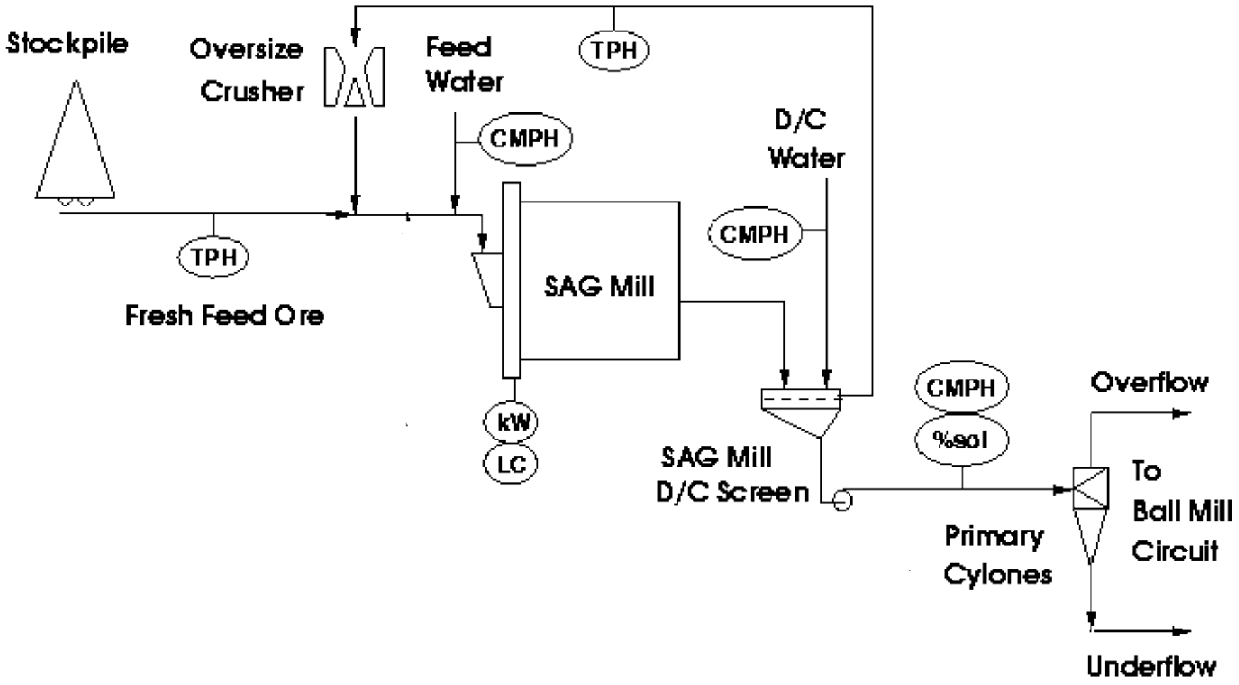

Figure 3. 1 – Schematic demonstration of the OT mine primary grinding circuit

3.2 Experimental design

In this study, the Kalman Filter algorithm was used to guide synchronous permanent magnet which has a marked-relation to the tumbling mill filling degree. The Kalman Filter (KF) is a wide range of algorithms for estimation and prediction, particularly when there is a lot of noise in the data. KF is used for a linear transition function, whereas in nonlinear transition using Extended Kalman filter (EKF). Unfortunately, in reality, we dealt with very seldom to the linear system – most systems are ultimately nonlinear. Even the simple relation I=V/R Ohm's Law is an approximation over a limited operating range. If the voltage is over a resistor exceeds a specific amount, then breaks down Ohm's Law. There were many papers about EXF, though few of them working algorithm of the filter. In our case, the working algorithm is used to show the simulation and illustration of the adjusting and accuracy of the model.

3.2.1 Kalman filter for state estimation

The KF is a recursive algorithm used to estimate a dynamic system that has a lack of data. The explanation for insufficient data is environment or noise, such systems, for instance,

involves: autonomous and assisted navigation system. It utilizes prior knowledge to predict the state of the system of the past, present as well as future. The KF has the advantage that the data are updated in each and every iteration so that we don't need much memory to save all data for system prediction. The only difference of KF and EKF are the we must linearize, non-linear function by applying the Jacobian matrix, then we can use the rest of the process KF algorithm (Keatmanee, Chadaporn, et al., 2014).

The Kalman Filter is a common recursive motion prediction algorithm, this simple application intended to predict the next bug movement position walking in a straight line. The Kalman filter theory is to consider the probability of the predicted state hypothesis is given by hypothesis of prior state and the use of measuring sensor data to correct the assumption of getting the best estimate for each time. In fact, applying KF has to consider model creation involving a model of state and measurement as shown in equation 3.1 and 3.2.

$$x_{k+1} = Ax + Bu_k + w_k \tag{3.1}$$

$$z_k = Hx_K + v_k \tag{3.2}$$

where:

- A, B and C are matrices
- k is the time index
- x is called the state of the system
- u is a known input to the system (called control signal)
- z is the measured output
- w and v are the noise – w is called the process noise, and v is called the measurement noise. Generally, each of these variables are vectors and therefore contains more than one element.

The first equation is a linear stochastic equation, which means that each x_k is estimated. The second equation indicates that any measured value, uncertain of its precision is a linear combination of the measuring noise, the signal value and both those are known as Gaussian. In the process, both noise and measurement noise are statistically independent.

Although the entities A, B and H are the general forms of matrices, in several of our signal processing problem models, we treat these entities as numerical values. Furthermore, even these values may change between states, then they can be assumed to be constant in the most

times. When we are confident our system firs in with this model, but in the first time which was difficult to be fitted, estimate mean and standard deviation of the noise functions w_k and v_k would be just the one thing left to do. Though in reality there is no signal in pure Gaussian form, but with some approximation, we can consider that. That won't pose a problem, because we will see the Kalman Filtering Algorithm attempts to converge into proper estimates, even if the parameters of Gaussian noise are poorly estimated.

The KF results from the constant updating of the estimates data based on prior knowledge in each iteration of filtering and prediction. In each iteration, the change is derived and interpreted within the Gaussian probability density function (pdf). KF associates the innovation process with the filter, that is the novel information prediction in noisy environment expressed by the state estimation by the usage of data in the last measurement of the system.

When either the dynamics of the system state (state model) or the dynamics of the observation (measurement model) is nonlinear, the conditional probability density functions which prove the minimum estimate of mean-square is no longer Gaussian. The optimal non-linear filter propagates the non-Gaussian functions and calculates their mean, which is a high burden on computation. A non-optimal approach solving problem in the frame of linear filter, which is called the Extended Kalman filter (EKF). The EKF establishes a KF for system dynamics that created from the linearization of the original non-linear filter, KF estimated of the previous state using the Jacobian matrix sometimes only call Jacobian.

3.3 Extended Kalman Filter

The most important part of applying EKF is the development of model use mathematical skills to construct a transitional function which is nonlinear in each state for unknow parameter estimate. There are two EKF models including state and measurement models.

State Model: $x_{k+1} = f(x_k, u_k + w_k)$ (3.3)

Where:

x - is the state model that consists of parameters used for prediction in each state.
x_{k+1} - is the next state from in which we get the predicted data from using transition function what is a non-linear function.
u_k - is the control data that is optional.
w_k - is Gaussian white noise

Measurement Model: $z_k = h(x_k + v_k)$ (3.4)

Where

z_k - is the measurement model which is consisting of parameters which data come from various kinds of sensors

v_k - is Gaussian white noise

The recursive algorithm method, EKF is depicted in Figure 3.1. there 2 main pars, with predictions and state of correction. Use $\hat{x}_{\bar{k}}$ and $P_{\bar{k}}$ are estimated from prediction state in which $\hat{x}_{\bar{k}}$ is obtained by utilizing state transition model and $P_{\bar{k}}$ is user-defined, for calculation of Kalman Gain or K is the confident value of state model and measurement variable. In the case of R approaching to 0, it means variable calculation is more accurate than the state model, on the other hand, if $P_{\bar{k}}$ is approached to 0, then its vice versa. Afterward, estimated values are updated based on K. The final step is that covariance error is updated for the next iteration. So that, all parameters are updated in every iteration, hence the predicted and estimated data are becoming more reliable. EKF's important feature is the linearization of non-linear function f and h with the Jacobian matrix which is nearly first-order derivative. The example of Jacobian matrix calculation for the state transition matrix is shown equation below:

$$A_{[i,\ j]} = \frac{df_{[i]}}{dx_{[j]}}(\hat{x}_k, u_k, 0) \quad (3.5)$$

The Jacobian matrix of functions $f_i(x_1,x_2, \ldots, x_n)$, $i = 1, 2,\ldots,n$ of real variable x_i is the determinant of a matrix of which ith row lists all the first-order partial derivative of the function $f_i(x_1,x_2, \ldots, x_n)$.

The estimated state model and measurement model values come from equations shown as follows:

$x_{k+1} =\sim \bar{x}_{k+1} + A(x_k - \hat{x}_k) + Wwk$ (3.6)

$z_k = \hat{z}_k + H(x_k - \hat{x}_k) + Vvk$ (3.7)

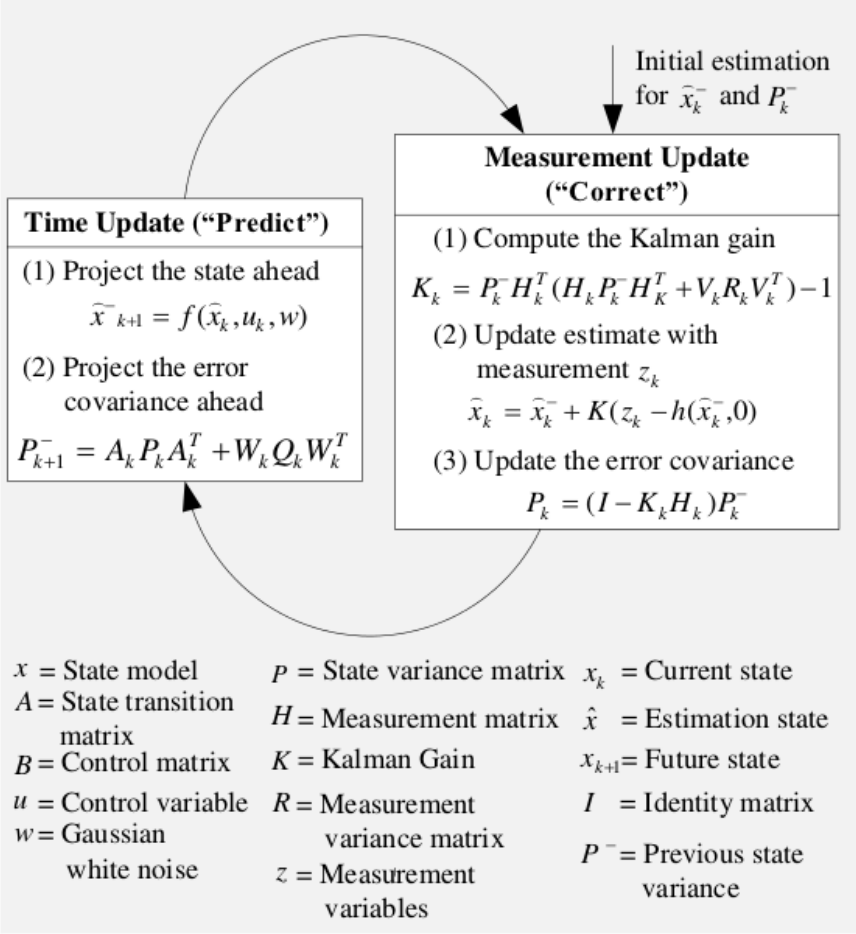

Figure 3. 2 – A complete process of the operation of the Extended Kalman Filter

3.4 Applying Kalman Filter

For implementing both KF and EKF, the knowledge of mathematics, statistics, and probability as well as physics are needed for creating a model that is the most important criterion. We want to measure x for state estimation problems since it includes all the details of the system. The problem is we can't measure x straight away. Instead of this, we measure z, which is a function of x corrupted by noise v. Then, we can use z to help us get an estimate of x; but we cannot take necessarily information from z because it's corrupted by noise.

Let's to consider the state estimate of permanent magnet synchronous motor. Which is used for high power required applications such as pump, compressor, rolling mill. Possibly we want to estimate the states because we want to know motor location or speed for some reason. Suppose we could calculate the motor winding currents. We could just use z_k as an estimate of our winding current, but z_k is noisy. By the way, using a Kalman filter we could do better. This is because a Kalman filter doesn't use only the winding current z_k but also the information contained in the state equation. The Kalman Filter equations expressed as follows:

$$K_k = P_k H^T (H P_k H^T + R)^{-1} \quad (3.8)$$

$$\hat{x}_{k+1} = (A\,\hat{x}_k + B u_k) + K_k(z_k - H\,\hat{x}_k) \quad (3.9)$$

$$P_{k+1} = A_k(I - K_k H)P_k A^T_k + Q \quad (3.10)$$

Where:

- k – is the time step (k = 1, 2, 3, ..);
- $\hat{x}_k$ – is the estimate of x_k
- K_k – is the Kalman filter gain (it is a matrix)
- P_k - is called estimation error covariance, which is also matrix
- Q – is the covariance of the process noise w_k, and R is the covariance of the measurement noise
- The *-1* superscript indicates matrix inversion
- The T superscript indicates matrix transposition
- I - is the identity matrix
-

3.4.1 Taylor series expansion

To linearize a nonlinear system, we are going to use a mathematical tool called the expansion of the Taylor series. The approach to nonlinear Kalman filtering is extending the nonlinear system equation in terms of Taylor series expansion around its nominal point $\bar{x}$. Taylor series expansion to nonlinear function expressed as follows:

$$f(x) = \sum_{n=0}^{\infty} \frac{f^n(\bar{x})\Delta x^n}{n!} \quad (3.11)$$

In the above equation,

- $\Delta x = x - \bar{x}$
- $f^n(\bar{x})$ – is the nth derivative of f(x), evaluated at x= $\bar{x}$

Linearizing a function means expanding it in a first-order Taylor series around some expansion point. In other words, the first-order Taylor series expansion of a function f(x) is equal to

$f(x) = f(\bar{x}) + f'(\bar{x})\Delta x$

Figure 3.3 shows the sin(x) function along with its expansion[5] of the first-order Taylor series around the nominal $\bar{x}$=0. Note that the two lines in the figure are fairly close for small values x, that shows the expansion of the Taylor series is a good approximation to sin(x). Even though, as x gets larger, the two lines diverge, meaning that the Taylor series is a poor approximation.

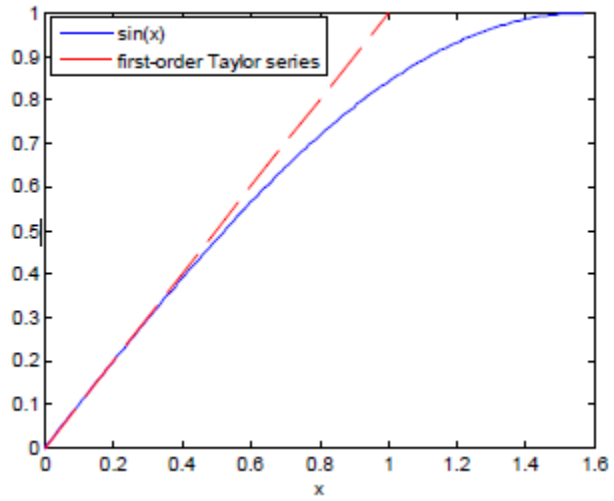

Figure 3. 3 – The first-order Taylor series expansion of sin(x) is accurate for small values of x, but becomes poor for larger values of x.

3.4.2 Extended Kalman filter algorithm

After making some substitutions to the linearized Kalman filter equations and going through some mathematical manipulations, we have the following the EKF algorithm.

1. The system equations are given as follows:

State equation: $x_{k+1} = f(x_k, u_k) + w_k;$
output equation: $z_k = h(x_k + v_k)$;

2. At each time step, compute the following derivative matrices, evaluated at the current state estimate:

$A_K = f'(\hat{x}_{k,} u_k)$

$H_k = h'(\hat{x}_k)$

Note that the derivatives are taken with respect to x_k, and then evaluated at $x_k = \hat{x}_k$.

Execute the following Kalman filter equations:

$K_k = P_k H^T (H P_k H^T + R)^{-1}$

$\hat{x}_{k+1} = (A\,\hat{x}_k + B u_k) + K_k(z_k - H\,\hat{x}_k)$

$P_{k+1} = A_k(I - K_k H)P_k A^T_k + Q$

3.5 Data analysis based on the data set of "OT" mine

Our main goal was to estimate ball filling degree of SAG mill based-on useable theoretical data of running mill. Firstly, we have explored available data and found their relation to the filling degree. Afterward, the most related data set was chosen and analyzed their coefficient correlation.

The following data are given by grinding process engineers and which are filtered values. Before analyzing data, we have to normalize it because these values are in different ranges. Furthermore, their correlation was estimated to find which parameters have a remarked influence to another one. Considering these dependencies to the filling degree of the mill to be assumed. In the table, SAG mill feed, load, speed, and power are more utilized values for the system designing.

Table 1: Ot mine SAG mill parameter data set, under the security permission only small part is shown

SAG Feed rate	SAG load	SAG speed	SAG power	SAG feed density	SAG bearing pressure
tonn/hr	tonn	rpm	kW	%	kPa
2073.510639	1047.837696	9.345433836	19383.02829	67.79556037	7717.624023
2081.099084	1052.813007	9.424890264	19262.43745	67.70033455	7717.624023
2067.416632	1044.470183	9.486808957	19308.018	67.56383669	7707.807367
2124.171136	1044.769921	9.484372273	19348.28548	67.72348932	7686.921387
2177.660055	1049.309761	9.481777245	19330.91049	67.66297875	7707.557729
2197.19909	1042.950982	9.502693575	19109.44291	67.63721235	7720.219238
2208.030984	1024.331944	9.513629101	18842.59073	67.57123924	7688.881682
2269.445573	990.641172	9.515053136	18481.55341	67.72519251	7614.831211
2330.174183	966.0506204	9.515006859	18710.71402	68.69539099	7540.524828

3.5.1 Data normalization

Data normalization is a process in which data attributes are organized within a data model to enhance the cohesion of the types of entities. In other words, the goal of data normalization is to reduce and even eliminate data redundancy, which is an important consideration for system designers and application developers because storing objects in a relational database that holds the same information in several places is incredibly difficult.

Secondly, normalization is a technique often applied as part of data preparation for system designing. The main goal of normalization is to adjust the values of numeric columns in the dataset to a specific scale, without distorting variations in the ranges. Although, every dataset doesn't require normalization for data analysis. Only when features have different ranges is required or different dataset needed to be analyzed within a specific range. In our

case, we have many data sets with different ranges, therefore data are normalized by the following equation to the desired range:

V = $\frac{v-\min(A)}{\max(A)-\min(A)}$ * (new_max– new_min) + new_min;

Where:

- V – is the normalized value
- v – is the specific value of the dataset
- min(A) – is the minimum value of the dataset
- $\max(A)$ – is the maximum value of the dataset
- new_max – is the new maximum range
- new_min – is the new minimum range

To initialize the Kalman filter, it is appropriate to start with and $\hat{x}_0$ of the state of at the initial value. We must also begin with an initial estimation error covariance P_0, which is our uncertainty about our initial estimation of the situation. If our initial estimate is $\hat{x}_0$ and we believe it then P_0 is to be very small. If our initial estimate is very uncertain $\hat{x}_0$, then P_0 is should be greater. In the long run, these initialization values in the filter won't make a big difference.

3.6 Correlation coefficient R

A coefficient of correlation is a numerical measure of some type of correlation, meaning a statistical relationship between two variables. The variables may be two columns of a given set of observations, often called a sampleor two components of a multivariate random variable with a known distribution. There are several types of the correlation coefficient, each with its definition and usability range and features.

How to interpret a Correlation Coefficient R?

The values are always between +1 and -1. To measure its meaning see which of the following values is nearest to your correlation R:

- Exactly – 1 is a perfect downhill linear relationship
- -0.70 is a strong downhill relationship
- -0.50 is a moderate downhill relationship
- -0.30 is a weak downhill linear relationship
- 0 is no linear relationship and the positive sign is vice versa.

3.6.1 Coefficient of determination R^2

In mathematics, the determination coefficient denoted as R^2 and pronounced "R squared" is the proportion of the variance in the dependent variable which is predictable from the independent variables. It is a statistic used in the context of statistical models, the main objective of which is either to anticipate future results or to test hypotheses, based on other similar facts. It provides a measure of how well the model replicates observed outcomes, based on the proportion of the total variation of outcomes explained by the model.

Chapter 4: Results and Discussion

Introduction

This chapter presents and addresses the results of experiments and simulations which were given in detail in Chapter 3. The first part of the chapter begins with the discussion of results on how synchronous motor control affects the filling level of the mill and which parameters of the motor are more sensitive to the control system. The next section covers many different theoretical data intermediate correlation and which one of them has a strong effect on filling level and mill performance. It also includes a discussion of the outcomes associated with mill power draw profiles during breakage of the ores.

4.1 State estimation of synchronous motor

Simon et al., (1968) modeled state estimation of the permanent magnet synchronous motor. They should want to estimate the states therefore, they can regulate them with a control algorithm and want to know the position or velocity of the motor for specific reasons. Then, they considered that to measure the motor winding currents and used the Extended Kalman filter (EKF) to calculate rotor position and velocity. The mathematical system equations are modeled as follows:

$$\dot{I} = \frac{-R}{L} I_a + \frac{w\lambda}{L} sin\theta + \frac{u_a + \Delta u_a}{L}$$

$$\dot{I} = \frac{-R}{L} I_b + \frac{w\lambda}{L} cos\theta + \frac{u_b + \Delta u_b}{L}$$

$$\dot{I} = \frac{-3\lambda}{2J} I_a sin\theta + \frac{3\lambda}{2J} I_b cos\theta - \frac{Fw}{J} + \Delta\alpha$$

$$\dot{\theta} = w$$

$$y = \begin{pmatrix} I_a \\ I_b \end{pmatrix} + \begin{pmatrix} v_a \\ v_b \end{pmatrix}$$

The variables in these equations are defined as follows:

- I_a and I_b are the currents in the two motor windings.
- θ and w are the angular position and velocity of the motor
- R and L are the motor winding's resistance and inductance.
- λ is the flux constant of the motor.
- F is the coefficient of viscous friction that acts on the motor shaft and its load.
- J is the moment of inertia of the motor shaft and its load.
- $u_a \ \ and \ u_b$ are the voltages that are applied across the two windings.
- Δu_a and Δu_b are noise terms due to the load torque.
- y is the measurement.

Here, we have assumed that we have measurements of the two winding currents. These measurements are deflected by measurement noises v_a and v_b, these noises are due to the sense resistance uncertainty, electrical noise, and quantization errors.

When we want to apply and EKF to the motor, then we need to identify the device states. To look at the system equations the state can be seen and note wherever a derivative appears. If it's a in the system equation variable is differentiated, then the quantity is equal to state. So, we can see from the above motor equations, our system has four states, and state vector x is expressed as follows:

$$x = \begin{bmatrix} I_a \\ I_b \\ w \\ \theta \end{bmatrix}$$

The system equation is obtained by discretizing the differential equations to

$x_{k+1} = f(x_k, u_k) + w_k$

$$= x_k + \begin{bmatrix} -\frac{Rx_k(1)}{L} + \frac{x_k(3)\lambda sinx_k(4)}{L} + u_{ak}/L \\ -\frac{Rx_k(2)}{L} + \frac{x_k(3)\lambda cosx_k(4)}{L} + u_{ak}/L \\ -\frac{3\lambda x_k(1)sinx_k(4)}{2J} + \frac{3\lambda x_k(2)cosx_k(4)}{2J} - Fx_k(3)/J \\ x_k(3) \end{bmatrix} \Delta t + \begin{bmatrix} \Delta u_{ak}/L \\ \Delta u_{ak}/L \\ \alpha \\ 0 \end{bmatrix} \Delta t$$

$z_k = h(x_k + v_k)$

$$= \begin{bmatrix} x_k(1) \\ x_k(2) \end{bmatrix} + \begin{bmatrix} v_{ak} \\ v_{bk} \end{bmatrix}$$

Where Δt is the step size that we're using for estimation in our microcontroller or DSP.

To use an EKF, we need to find the $f(x_k, u_k)$ and $h(x_k)$ derivatives respect to x_k. This is a new twist since both $f(x_k, u_k)$ and $h(x_k)$ are vectors functions of vector x_k. Then how can we find a derivative of a vector of respect to another vector? When we know the derivation method it is not difficult to calculate. For instance, if we write vectors x and f as follows:

$$f = \begin{bmatrix} f_1 \\ f_2 \\ f_3 \\ f_4 \end{bmatrix} \qquad x = \begin{bmatrix} x_1 \\ x_2 \\ x_3 \\ x_4 \end{bmatrix}$$

then the derivative od f with respect to x is equal to 4 x4 matrices.

$$f'(x) = \begin{bmatrix} df_1/dx_1 & df_1/dx_2 & df_1/dx_3 & df_1/dx_4 \\ df_2/dx_1 & df_2/dx_2 & df_2/dx_3 & df_2/dx_4 \\ df_3/dx_1 & df_3/dx_2 & df_3/dx_3 & df_3/dx_4 \\ df_4/dx_1 & df_4/dx_3 & df_4/dx_3 & df_4/dx_4 \end{bmatrix}$$

Then this can be generalized for any size of vector f and x. with this statement, we find the derivative matrices as follows:

$A_K = f'(\hat{x}_k, u_k)$

$$= \begin{bmatrix} -R/L & 0 & \lambda sin\hat{x}_k(4)/L & \hat{x}_k(3)cos\hat{x}_k(4)/L \\ 0 & -R/L & \lambda cos\hat{x}_k(4)/L & \hat{x}_k\lambda sin\hat{x}_k(4)/L \\ -3\lambda sin\hat{x}_k(4)/2J & 3\lambda cos\hat{x}_k(4)/2J & -F/J & 3\lambda[\hat{x}_k(1)cos\hat{x}_k(4) + \hat{x}_k(2)2sin\hat{x}_k(4)]/2J \\ 0 & 0 & 1 & 0 \end{bmatrix}$$

$H_k = h'(\hat{x}_k)$

$$= \begin{bmatrix} 1 & 0 & 0 & 0 \\ 0 & 1 & 0 & 0 \end{bmatrix}$$

Now, let's simulate the EKF and to see how well we can estimate the velocity and rotor location. We must assume that the noise levels, $v_{bk}\ and\ v_{ak}$, are zero-mean variables with a standard deviation of 0.1amps. The winding voltages are equal to:

$u_a(t) = sin2\pi t$

$u_b(t) = cos2\pi t$

This means that in discrete time, the control inputs are equal to:

$u_{ak} = sin2\pi\Delta t$

$u_bk = cos2\pi\Delta t$

The voltages applied to the winding currents are the same as those plus Δu_{ak} and $\Delta u_{bk,}$ which are zero-mean variables with default derivations of 0.001 amps. The noise $\Delta\alpha_k$ has a standard deviation of 0.05 rad/sec^2 due to load torque disturbances. In spite of this, our measurements consist only of winding currents, by using EKF the rotor position and velocity are estimated. For the simulation, Matlab code was used and the EKF code listing is attached appendix section end of this study. The simulation results are shown in Figure 3.4 For that we can see that the rotor position and velocity are calculated very reasonably.

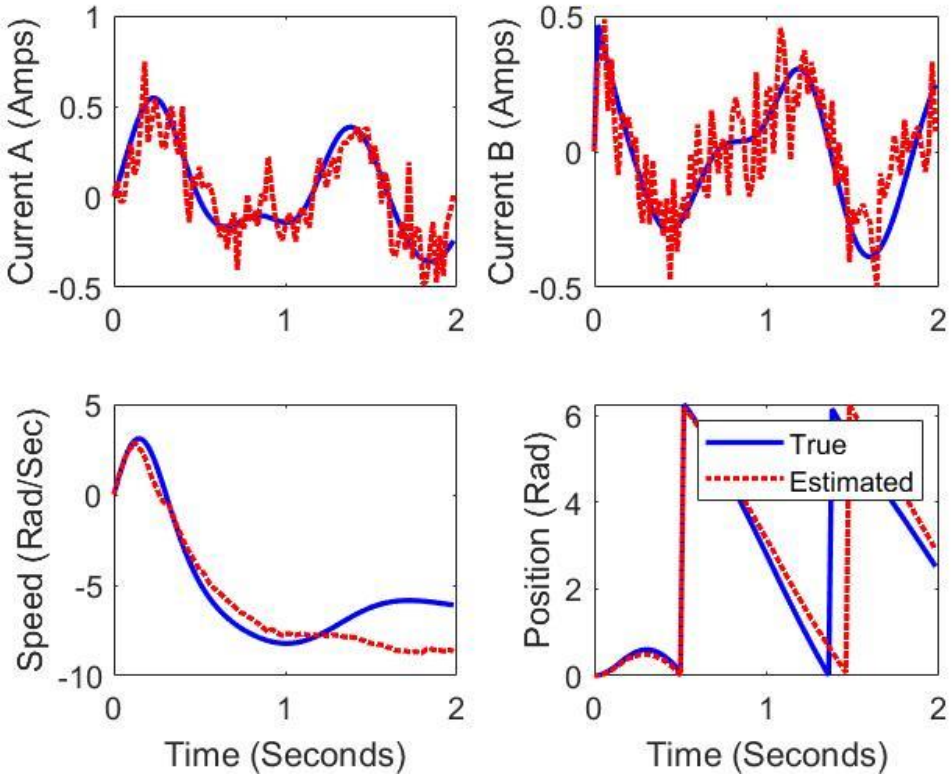

Figure 4. 1 - Extended Kalman filter simulation results for a permanent magnet synchronous motor. Winding current measurements are obtained once per millisecond.

In practical terms, this means we can evaluate the position and velocity of the rotor without using the encoder. We just need a few sense resistors instead of an encoder to get a rotor position and Kalman filter in the microcontroller. This is an outstanding example of a trade-off both mathematics and instrumentation. if we know how to apply given mathematics of Kalman filter in a microcontroller, we can then get rid of our encoder and save a lot of money in our embedded systems product.

How the Extended Kalman filter makes sense for ball filling?

In a state estimation of the synchronous motor, there are several parameters are considered constant. Only three parameters are variable to control motor which are acceleration noise, control noise, and measurement noise. The measurement nose also to be constant because it depends on type tool or equipment measuring specific parameter and it is considered based on the standard. Therefore, how can we use control noise and acceleration noise to our ball measurement? In our grinding system, we are measuring power-draw in terms of currents and voltages were constant. Power is correlated with other mill parameters, in this case assuming those factors motor is controlled by using extended Kalman filter. For the power regulation, the control noise term is used and acceleration noise is an additional term. It comes from, when motor transfer motion to the shaft, then shaft rotates mill. On the other-hand, this noise comes from mechanical work.

4.2 Correlation coefficient of mill parameters

As described previous chapter correlation coefficients of several SAG mill parameters estimated as follows by Matlab coding. As shown in Table 2 some parameters have a really good relationship which was used for further data analysis. The highest relevance (R=0.9687 blue color) is found between SAG load and bearing pressure because these two parameters are two sides of the coin. One is expressed by the ton and the other one is by pressure although, there is a small amount of variation around 3 percent. Which is considered as measurement uncertainty? The next correlation is founded that between SAG load and power-draw which is 0.82862 (depicted by yellow color) and R-squared is 6866. This value expresses a very reasonable correlation and it is used for further ball addition estimation.

Table 2: Correlation coefficient of different parameters shown in the table estimated by Matlab.

column/row	1	2	3	4	5	6	7
1	1	0.098622	-0.00292	0.33143	0.19055	-0.06239	-0.10488
2	0.098622	1	-0.4211	-0.27112	-0.54283	0.41024	-0.47672
3	-0.00292	-0.4211	1	0.38238	0.82863	-0.30239	0.96876
4	0.3314	-0.27112	0.38238	1	0.64672	-0.23542	0.36849
5	0.19055	-0.54283	0.82863	0.64672	1	-0.33562	0.78634
6	-0.06239	0.41024	-0.30239	-0.23542	-0.33562	1	-0.32647
7	-0.10488	-0.47672	0.96876	0.36849	0.78634	-0.32647	1

4.2.1 General correlation of mill parameters

In this section a general relation of important SAG mill parameters expressed and some of them are inversely proportional or directly proportional. As shown in figure 4.2 SAG mill speed, power, and load are directly proportional. Although in the beginning of the graph, there is a variation of speed, then it is considered measurement error. Because the principle of SAG mill controlling these three parameters has to be directly proportional ignoring some special cases. To compare these different range values, data were normalized between 0 to 1 by y-axis.

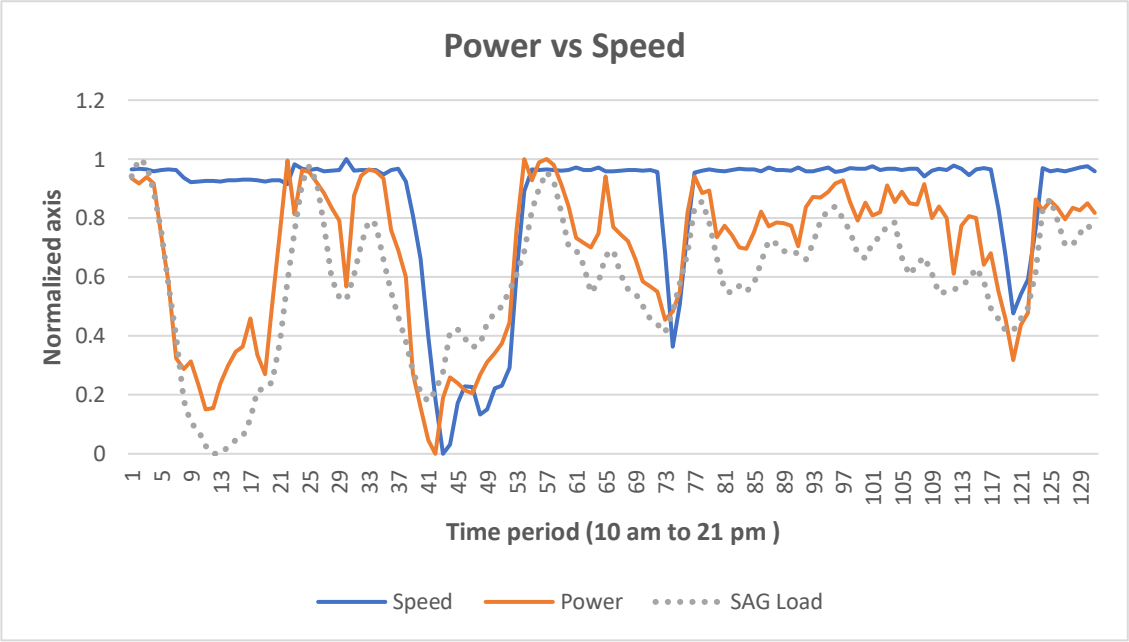

Figure 4. 2 – General correlation overview of SAG mill important parameters

Figure 4.3 is one of the interesting graphs and gives the key point of further experiments. As shown in the graph feed rate (tph) and power-draw are inversely proportional, which leads us a more concentrating relationship between ball addition and power. Stated earlier that “OT” SAG mill charge takes up to 33-35 percent of the mill volume. Grinding balls occupy up to 18-20 percent of the mill volume, which means that it is around 55 percent of the total charge, as well as density of the steel balls, are much larger than the density of ores. Therefore, the feed rate has a lower influence to the power-draw. This gives us one vital validation for the future ball filling analysis.

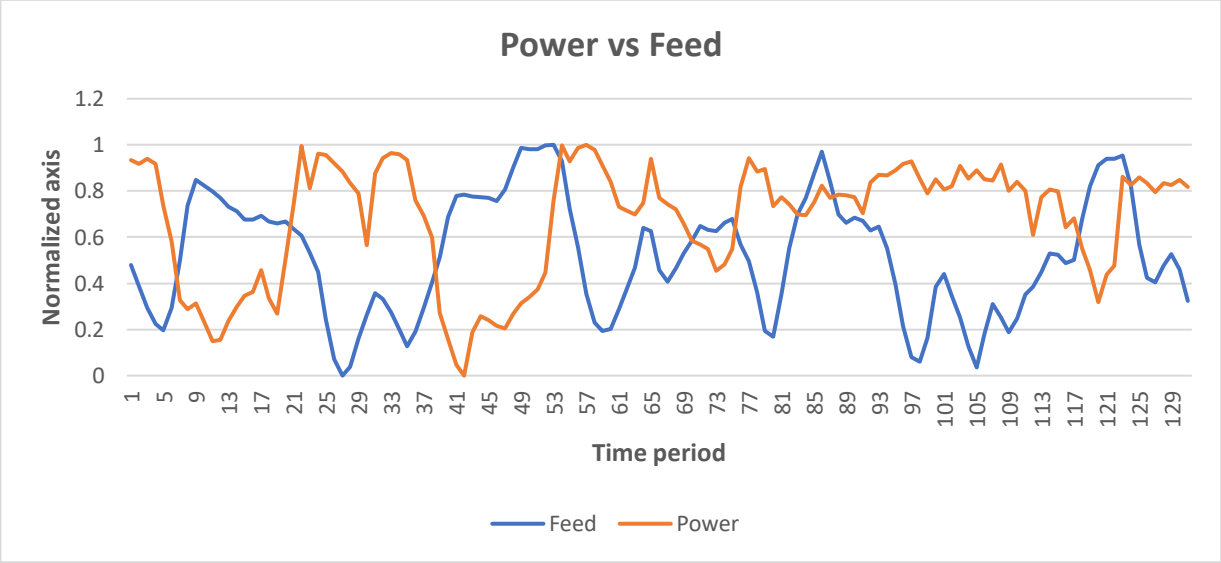

Figure 4. 3 – Relationship between mill power-draw [kW] and feed rate [tph]

4.3 Correlation coefficients used for ball addition

We have three days data set of the above-mentioned parameters of SAG mill and after that correlation of those values were estimated respectively. Power-draw and SAG load have a satisfactory correlation determination or R-squared = 0.6866 this value derived from three days of data. At the OT mine ball charge is added twice a day in the morning and evening. By using, this information we have calculated R-squared between those ranges respectively. For this study, three different cases used in which 25 tons, 15 tons, and 5 tons ball addition correlation determinations were evaluated. Correlations of these conditions were estimated and then those values were compared to the total R-squared valued to predict threshold value for the ball addition.

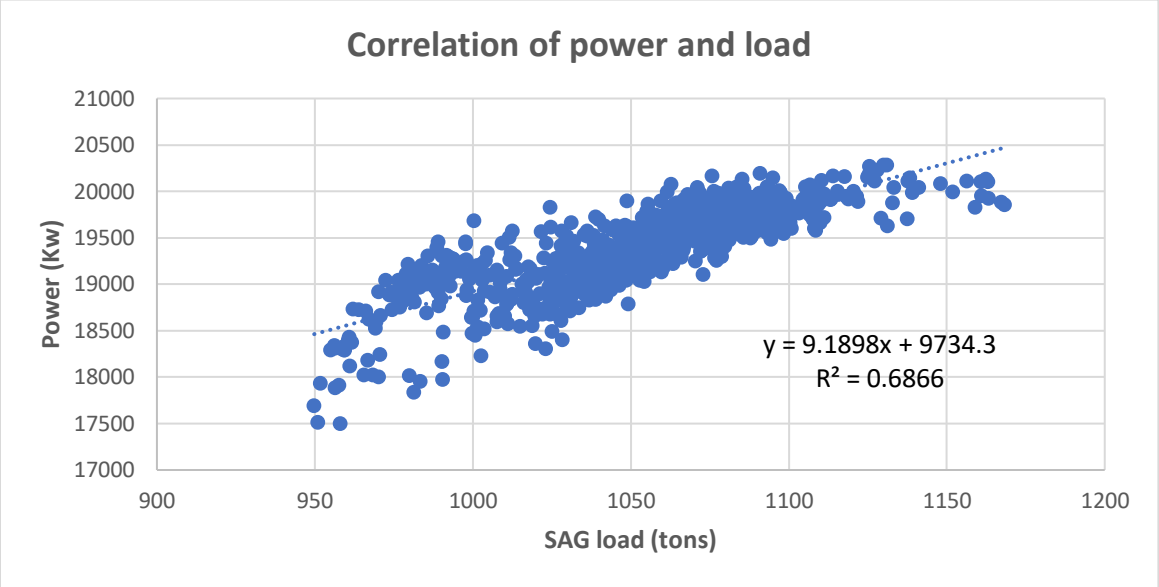

Figure 4. 4 – Correlation determination (r-squared) value of three days data

4.3.1 The experiment of 25 tons ball addition

We have calculated an R-squared value of 25 tons of ball addition in two different cases. The first case is using data from 25 tons balls charge to the next ball charge period (it is mostly 12 hours), in this case, R-squared is equal to 0.76 which really good result. This value greater than the general determination coefficient (R^2=0.68) and it is around 7 percent deflection. The second case is to calculate the correlation determination during the ball charging period which expresses a high correlation than the total R^2 value of the specific range. At 25 tons ball addition case it takes around 3.5 hours because OT mine grinding circuit ball is added one by one to the ore feeding conveyor belt. Moreover, this value is around 3.5 percent larger than the total R^2 of 25 tons ball addition and 10.5 percent larger than the general R^2 value.

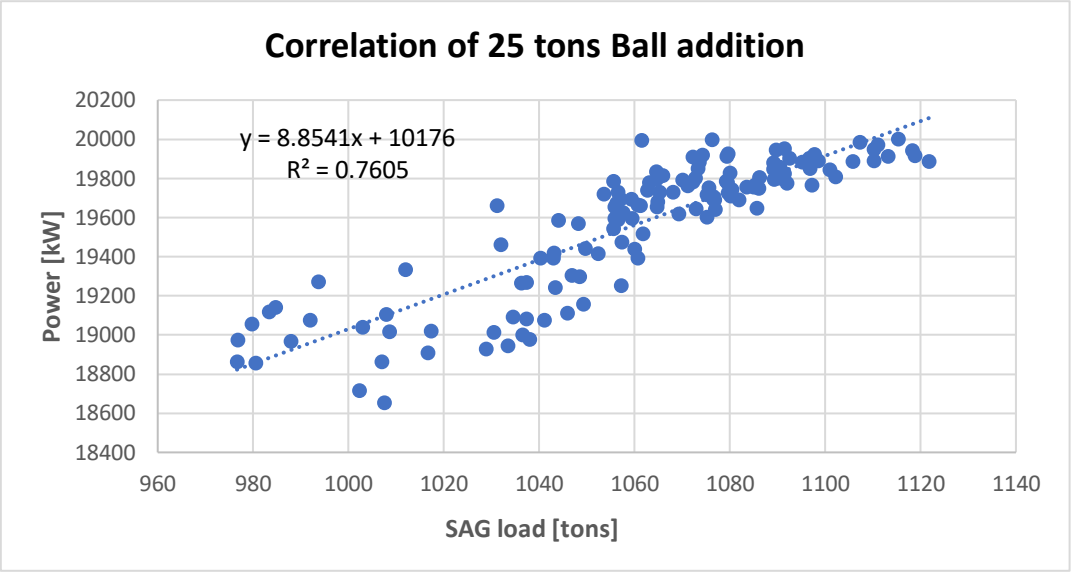

Figure 4. 5 – Correlation determination (r-squared) value at specific state (25 tons ball addition)

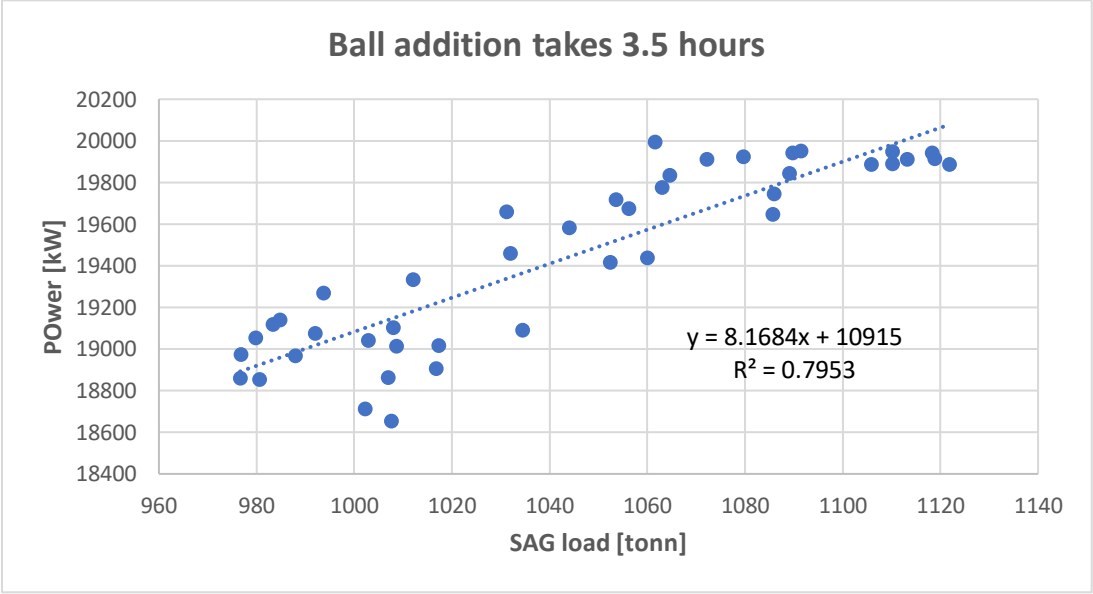

Figure 4. 6 – Correlation determination (r-squared) value of during ball charging period (at 25 tons ball addition)

4.3.2 The experiment of 15 tons ball addition

In two different cases, we calculated an R-squared value of 15 tons of ball addition. The first case uses data from 15 tons of ball feed to the next ball feed period (it also nearly 12 hours), int this case R-squared is equal to 0.67 which is a really good result. This is greater than the coefficient of general determination (R^2=0.68), and is about 1 percent deflection. In the second case is to calculate the ball charging R^2 only considering the charging period as same as the previous experiment. Which introduces a high correlation than the total R^2 value of a specific range. It takes about 2 hours at 15 tons ball addition. In addition, this value is around 7 percent larger than the total R^2 at 25 tons ball addition and 6 percent larger than the general R^2 value.

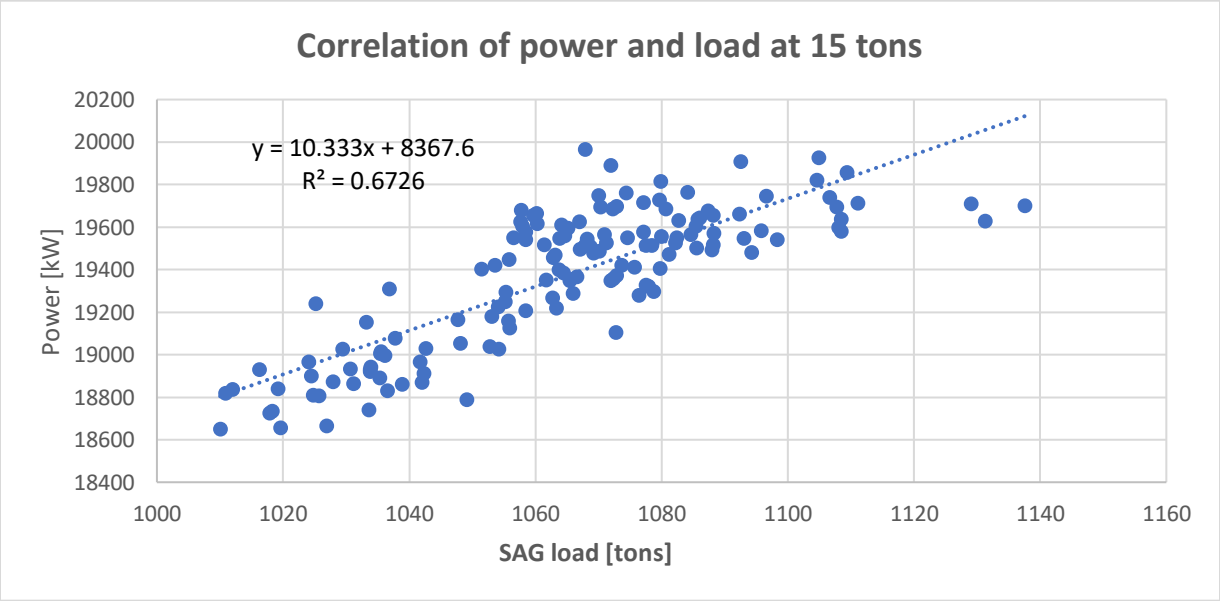

Figure 4. 7 – Correlation determination (r-squared) value at specific state (15 tons ball addition)

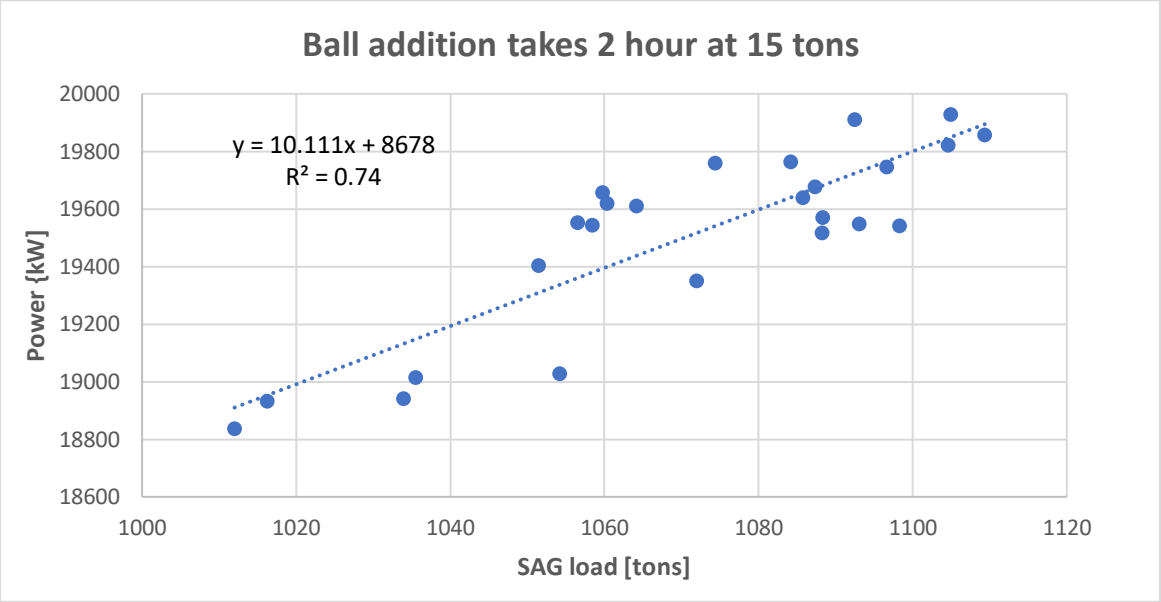

Figure 4. 8 – Correlation determination (r-squared) value of during ball charging period (15 tons feeding takes around 2 hours)

4.3.3 The experiment of 5 tons ball addition

In two different cases, we calculated an R-squared value of 5 tons of ball addition. The first case uses data from 15 tons of ball feed to the next ball feed period (it also nearly 12 hours), int this case R-squared is equal to 0.76 which is a really good result. This is greater than the coefficient of general determination (R^2=0.68), and is about 5 percent deflection. The second case is to calculate the ball charging R^2 only considering the charging period as same as the previous experiment. Which introduces a high correlation than the total R^2 value of a specific range. It takes about 1 hour at 5 tons ball addition. In addition, this value is around 5 percent larger than the total R^2 at 25 tons ball addition and 13 percent larger than the general R^2 value.

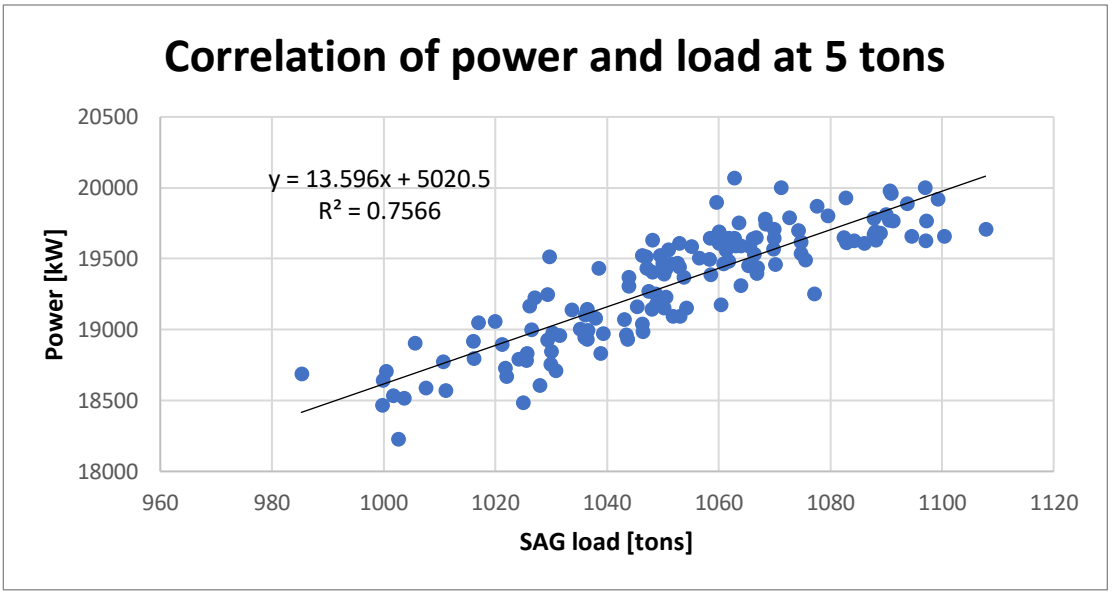

Figure 4. 9 – Correlation determination (r-squared) value at specific state (5 tons ball addition)

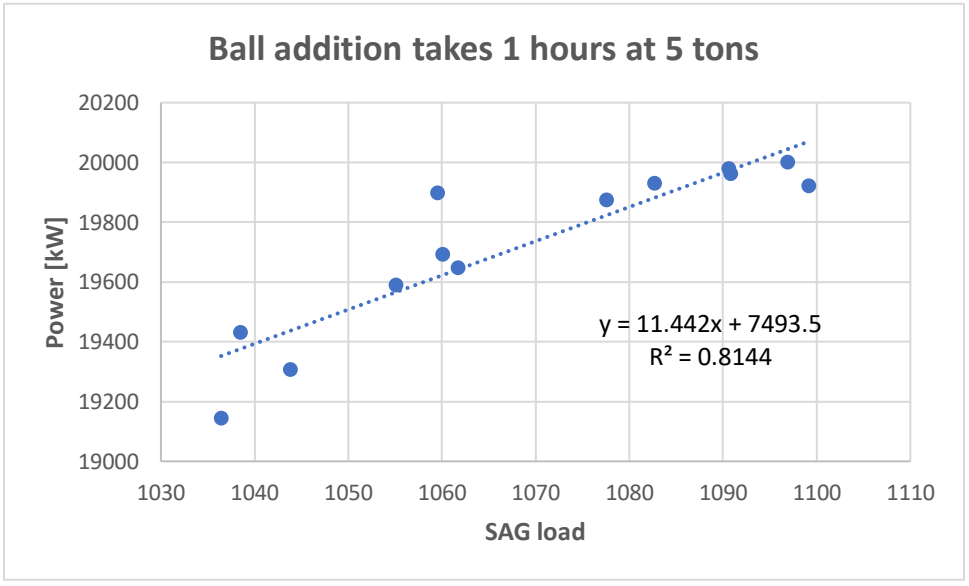

Figure 4. 10 – Correlation determination (r-squared) value of 5 tons ball addition take up to 1 hour

To conclude the above three experiments the following results we can get. To revise the ball addition sequence of OT grinding circuit at above three cases firstly 25 tons ball added after 12 hours 5 tons ball added as well as after 12 hours 15 tons balls were added. Currently, OT

engineers are adding ball measures between 5 tons to 25 tons based on the daily grinding process throughput. In our experiment based on R^2 values, we have designed reasonable ranges for ball addition. 25 tons of balls added to SAG mill after 12 hours coefficient of determination is 0.76 and it greater than general R^2 values which means in the circuit has a possible amount of ball load. This is one embodiment of research. Secondly, the difference between R^2 value of 25 tons ball addition and R^2 of during charging value difference only 3.5 percent, which indicates that there is less ball wear rate. Sometimes it is due to the hardness of ores and which is the second embodiment of research. In this case, we assumed that adding ball size between 5 tons – 10 tons, on the OT data sequence they added 5 tons of ball. Then 5 tons of balls added to the grinding process, after 12 hours specific R^2 is 0.75 and which is considered quite well. However, the difference of specific R^2 and R^2 during the charging period is 6 percent, it seems to be quite considerable value. In this case, OT engineers added 15 tons of balls and agree with this amount because our one embodiment is not fulfilled. Then we assumed ball addition range between 10 tons to 15 tons. After adding 15 tons of ball experiment conducted out as described above, then the difference of specific R^2 and R^2 during the charging period is 7 percent. It is similar to the previous step then 15 tons of balls added and OT engineers did the same assumption.

Chapter 5: Conclusions and Recommendations

5.1 Summary of the research

This study helps to develop the methods for the continuous control of tumbling mills especially SAG mills. A promising method for estimating ball charge measurement has been studied, where a filtered theoretical data were used on the running mill.

The main idea of this thesis is to use available data set at the OT mine grinding circuit. By following the primary objective data analysis method was implemented. Firstly, we have researched more related data to the ball addition measurement. At the meantime, their correlation coefficients were calculated. As a result, the power-draw and load of SAG mill have favorable correlation determination values which are also called r-squared (R^2 = 0.68). Hence, to estimate more accurate ranges or values we have considered different conditions. For instance, at OT mine balls are added in the morning and evening with different sizes. The size variation is depending on many different variables. In this study, we calculated R^2 of each state and predicted ranges based on those values. We have gotten following ranges ball addition if the variation of r-squared value at the total specific state and r-squared value of during charge time is between 2 – 4 percent then we can add 5 tons – 10 tons of ball, at the same time we also have to consider the general r-squared value of grinding circuit. If the variation is between 4 -7 percent then we add 10 to 15 tons ball. To make a more accurate range we need as many data and as many experiments. This is one of the possible embodiments of analyzing available theoretical data of running SAG mill. we might think that, if we use this method with other different methods simultaneously, then we get a precise-results.

The second novel invention is using Kalman filter for controlling dynamics within in the SAG mill by regulating its motor. in practice, most systems are in a non-linear state. We've seen how in the non-linear systems, the Kalman filter can be modified for state estimation. The resulting filter is called the Extend Kalman filter. In this study, we described the discrete-time EKF. This is the kind of EKF we used if the system description is in discrete-time. There are also different possible options of Kalman filter depends on the requirements. If the system equations are continuous-time and the even measurements are continuous-time, so we can use continuous-time EKF. If the system equations are continuous-time and the measurements are discrete, then we can use hybrid EKF.

The importance of using an EKF is to be able to describe the system in a mathematical model. That is the EKF designer must understand the system reasonably well to be able to describe differential equations of its behavior. In practice, this is often the hardest part of applying of Kalman filter. Another difficulty of Kalman filtering is the ability to model the noise in the system. In the previous example of the motor controlling we assumed the measurement noises were zero-mean with a standard deviation of 0.1 amps. The only way to do it find out this if we know how sensitive our sense resistors are and whether you have a strong one knowing the electrical noise and discretization errors that corrupt the winding current measurement.

The derivation of the EKF in this research, the first-order Taylor series were used to approximate the non-linear equations of the system. If we use second-order Taylor series expansion then we get a more accurate approximation to our nonlinear equations. Higher-order approaches can provide better results if the non-linear expression is even difficult. Higher-order approaches involve second-order Kalman filter, iterated Kalman filter, grid-based Kalman filter. These filters provide ways of minimizing the errors in linearization which are part of the EKF. Those filters usually show performance estimation which is better than the EKF but more complicated and they needed a lot of computation. Other popular nonlinear state estimators including unscented Kalman filter and particle filter.

5.2 Future work

The next step will be implementing the sensor-based technology for the control and optimization of a SAG mill circuit for mineral processing. Because many innovative technologies easily measure the dynamic motion of the system. This involves further development in decreased power consumption for the sensor, telemetry system (wireless sensor), and data pretreatment methods for signal processing as we all compressing data.

To achieve greater accuracy in DEM predictions used and allow for quantitative comparison with measured data some important developments have been identified. This involves showing all load motion within the mill, simulation of time-dependent behavior of charge, and extension of the approach to a three-dimensional DEM mill model.

While there will still be opportunities for further validation of the models, the database is assumed to be extensive and broad enough to provide definitive evidence that several models can predict the tumbling mill fill level with relatively high precision. It is assumed that within the limits of data measurement error, changes to the predictive capabilities of the models can only be achieved at the strict limits of mill operating conditions.

Reference

Royston, D. *Semi-Autogenous Grinding (SAG) Mill Liner Design and Development Shell Liners*. no. 3, 2008.

Bureau, International. *Intellectual Property Organization International Bureau (43) International Publication Date 18*. no. August, 2011.

Clermont, B., and B. De Haas. "Optimization of Mill Performance by Using Online Ball and Pulp Measurements." *Journal of the Southern African Institute of Mining and Metallurgy*, vol. 110, no. 3, 2010, pp. 133–40.

Engineering, Chemical, et al. *INFERENTIAL MEASUREMENT OF SAG MILL PARAMETERS* T.A. APELT*", S.P. ASPREY" and N.F. THORNHILL** **. no. 6, 2006, pp. 575–91.

Goyena, Rodrigo, and A. .. Fallis. "**済無**No Title No Title." *Journal of Chemical Information and Modeling*, vol. 53, no. 9, 2019, doi:10.1017/CBO9781107415324.004.

H, Wilber Churata, and Minera San Cristobal S. A. *SAG AND BALL MILL ONLINE BALL CHARGE LEVEL MEASUREMENT BY SOUND Keywords*. pp. 0–11.

Jonsén, Pär, et al. "Prediction of Mill Structure Behaviour in a Tumbling Mill." *Minerals Engineering*, vol. 24, no. 3–4, Elsevier Ltd, 2011, pp. 236–44, doi:10.1016/j.mineng.2010.08.012

Keatmanee, Chadaporn, et al. "Simple Example of Applying Extended Kalman Filter Simple Example of Applying Extended Kalman Filter." *1st International Electrical Engineering Congress*, no. March, 2014.

Mill, Concentrator S. A. G., et al. *A Method to Determine the Ball Filling , in Miduk Copper Concentrator SAG Mill*. no. 1, 2012, pp. 15–19.

MORRELL, S., 1993. The prediction of power draw in wet tumbling mills.

Moys, H. "Model of Mill Power as Affected by Mill Speed, Load Volume and Liner Design." *International Journal of Rock Mechanics and Mining Sciences & Geomechanics Abstracts*, vol. 31, no. 2, 1994, p. A94, doi:10.1016/0148-9062(94)93077-5.

Napier-Munn, Tim, and Barry A. Wills. "Wills' Mineral Processing Technology." *Wills' Mineral Processing Technology*, no. October, 2005, doi:10.1016/B978-0-7506-4450-1.X5000-0.

Napier-Munn, T. J., et al. *Mineral Comminution Circuits Their Operation and Optimisation*. 1996, p. 413.

Núñez, Felipe, et al. “Characterization and Modeling of Semi-Autogenous Mill Performance under Ore Size Distribution Disturbances.” *IFAC Proceedings Volumes (IFAC-PapersOnline)*, vol. 44, no. 1 PART 1, 2011, pp. 9941–46, doi:10.3182/20110828-6-IT-1002.02199.

Owen, Phil, and Paul W. Cleary. “The Relationship between Charge Shape Characteristics and Fill Level and Lifter Height for a SAG Mill.” *Minerals Engineering*, vol. 83, Elsevier Ltd, 2015, pp. 19–32, doi:10.1016/j.mineng.2015.08.009.

Powell, M. S., et al. “DEM Modelling of Liner Evolution and Its Influence on Grinding Rate in Ball Mills.” *Minerals Engineering*, vol. 24, no. 3–4, Elsevier Ltd, 2011, pp. 341–51, doi:10.1016/j.mineng.2010.12.012.

Rowland, C.A “Using the Bond index to measure operating comminution efficiency.” *Mineral & Metallurgical Processing* 15, no. 4 (1998): 32-36.

Sarpong Bismark Donkor, by. *On-Line Sensors for Measuring the Total Ball and Charge Level in Tumbling Mills University of Cape Town Centre for Minerals Research*. 2014

Simon, Dan, and Dan Simon. “Review of Kalman Filters.” *Ieee Transactions On Automatic Control*, vol. 13, no. 1, 1968, pp. 83–86.

Tano, Kent. *Continuous Monitoring of Mineral Processes with Special Focus on Tumbling Mills – A Multivariate Approach*. 2005, p. 129, doi:1402-1544.

Usman, Husni. *Measuring the Efficiency of the Tumbling Mill As a Function Of*.

Yuan, Chengzhi, and Fen Wu. “Robust Control of Switched Linear Systems via Min of Quadratics.” *ASME 2013 Dynamic Systems and Control Conference, DSCC 2013*, vol. 1, 2013, doi:10.1115/DSCC2013-3715.

Appendix

Matlab codes for estimating correlation coefficient

```
Ndata=load('NormData.txt');
format shortg
[r,c]=size(Ndata);
 rS=zeros(c,c);
rA=zeros(c,c);
 for n=1:c
    figure (n)
     for m=1:c
         rA(n,m)=  r_analysis_array(Ndata(:,m),Ndata(:,n));
         rS(n,m)= rA(n,m).^2;
         txt =['[',num2str([n m]), ']', blanks(5),
'R^2=',num2str(rS(n,m))];
         plot(Ndata(:,m),Ndata(:,n),'*','LineWidth',2,
'DisplayName',txt) ;
         legend show;
         box off
         display([n m]);
         pause
     end
 end
xD=linspace(1,c,c);
bk=[blanks(1),blanks(1),blanks(1),blanks(1),blanks(1),blank
s(1),blanks(1)];
bk5=[bk' bk' bk' bk' bk'];
disp('Correlation R');
disp([blanks(13),num2str(xD(1)),blanks(17),num2str(xD(2)),b
lanks(17),num2str(xD(3)),blanks(18),num2str(xD(4)),
blanks(19),num2str(xD(5)),blanks(20),num2str(xD(6)),blanks(
15),num2str(xD(7))]);
display([num2str(xD'),bk5,num2str(rA(:,1)),bk5,num2str(rA(:
,2)),bk5,num2str(rA(:,3)),bk5,num2str(rA(:,4)),bk5,num2str(
rA(:,5)) ,bk5,num2str(rA(:,6)),bk5,num2str(rA(:,7))]);
disp('Correlation R^2');
disp([blanks(13),num2str(xD(1)),blanks(17),num2str(xD(2)),b
lanks(17),num2str(xD(3)),blanks(18),num2str(xD(4)),
blanks(19),num2str(xD(5)),blanks(20),num2str(xD(6)),blanks(
15),num2str(xD(7))]);
```

```
display([num2str(xD'),bk5,num2str(rS(:,1)),bk5,num2str(rS(:
,2)),bk5,num2str(rS(:,3)),bk5,num2str(rS(:,4)),bk5,num2str(
rS(:,5)) ,bk5,num2str(rS(:,6)),bk5,num2str(rS(:,7))]);
```

For array analysis

```
function  r_squared= r_analysis_array(x,y)
s=size(x);
r=s(1);
sumx=sum(x);
sumy=sum(y);
xSQRT=zeros(r,1);
ySQRT=zeros(r,1);
 xyMULT=zeros(r,1);
for i=1:r
    xSQRT(i)=x(i).^2;
    ySQRT(i)=y(i).^2;
    xyMULT(i)=x(i).*y(i);
end
sumxSQRT=sum(xSQRT);
sumySQRT=sum(ySQRT);
sumxyMULT=sum(xyMULT);
Num_r_squared=r*sumxyMULT-sumx*sumy;
Den_r_squared=sqrt((r*sumxSQRT-sumx^2)*(r*sumySQRT-
sumy^2));
r_squared=Num_r_squared/Den_r_squared;
display(r_squared);
end
```